JOURNAL OF PROTEOMICS 75 (2012) 3158–3176

Available online at www.sciencedirect.com

SciVerse ScienceDirect

www.elsevier.com/locate/jprot

Proteomic and redox-proteomic analysis of berberine-induced cytotoxicity in breast cancer cells

Hsiu-Chuan Chou[a], *Ying-Chieh Lu*[b], *Chao-Sheng Cheng*[b], *Yi-Wen Chen*[b], *Ping-Chiang Lyu*[b], *Cheng-Wen Lin*[c,*], *John F. Timms*[d,*], *Hong-Lin Chan*[b,*]

[a]*Department of Applied Science, National Hsinchu University of Education, Hsinchu, Taiwan*
[b]*Institute of Bioinformatics and Structural Biology & Department of Medical Science, National Tsing Hua University, Hsinchu, Taiwan*
[c]*Department of Medical Laboratory Science and Biotechnology, China Medical University, Taichung, Taiwan*
[d]*EGA Institute for Women's Health, University College London, London, UK*

ARTICLE INFO

Article history:
Received 30 November 2011
Accepted 8 March 2012
Available online 21 March 2012

Keywords:
Berberine
Proteomics
2D-DIGE
MALDI-TOF
Breast cancer
Redox proteomics

ABSTRACT

Berberine is a natural product isolated from herbal plants such as *Rhizoma coptidis* which has been shown to have anti-neoplastic properties. However, the effects of berberine on the behavior of breast cancers are largely unknown. To determine if berberine might be useful in the treatment of breast cancer and its cytotoxic mechanism, we analyzed the impact of berberine treatment on differential protein expression and redox regulation in human breast cancer cell line MCF-7 using lysine- and cysteine-labeling two-dimensional difference gel electrophoresis (2D-DIGE) combined with mass spectrometry (MS). This study demonstrated that 96 and 22 protein features were significantly changed in protein expression and thiol reactivity, respectively and revealed that berberine-induced cytotoxicity in breast cancer cells involves dysregulation of protein folding, proteolysis, redox regulation, protein trafficking, cell signaling, electron transport, metabolism and centrosomal structure. Our work shows that this combined proteomic strategy provides a rapid method to study the molecular mechanisms of berberine-induced cytotoxicity in breast cancer cells. The identified targets may be useful for further evaluation as potential targets in breast cancer therapy.

1. Introduction

Berberine is a natural product isolated from herbal plants such as *Rhizoma coptidis* and shown to be non-toxic to humans [1]. It has long been used to reduce inflammation [2], neutralize toxicity [3] and exhibit anti-bacterial activity [4]. Berberine has also been reported to show anti-tumor and inhibitory effects on hepatoma [5], esophageal cancer [6], colon cancer [7], breast cancer [8] and prostate cancer [9] via blockade of the cell cycle, inhibition of DNA synthesis, activation of caspases and induction of apoptosis. It has also been demonstrated that berberine acts as an anti-metastatic drug in human lung cancer via decreased production of urokinase-plasminogen activator and matrix metalloproteinase-2 [10]. Recently, the generation of

Abbreviations: 1-DE, one-dimensional gel electrophoresis; 2-DE, two-dimensional gel electrophoresis; Ab, antibody; BBR, berberine; BSA, bovine serum albumin; CCB, colloidal Coomassie blue; CHAPS, 3-[(3-cholamidopropyl)-dimethylammonio]-1-propanesulfonate; DCFH-DA, 2,7-dichlorofluorescin diacetate; ddH_2O, double deionized water; DIGE, differential gel electrophoresis; DTT, dithiothreitol; EDTA, ethylenediaminetetraacetic acid; FCS, fetal calf serum; MALDI-TOF MS, matrix assisted laser desorption ionization-time of flight mass spectrometry; NP-40, Nonidet P-40; SDS, sodium dodecyl sulfate; TFA, trifluoroacetic acid.

* *Corresponding authors.*
E-mail address: hlchan@life.nthu.edu.tw (H.-L. Chan).

1874-3919/$ – see front matter © 2012 Elsevier B.V. All rights reserved.
doi:10.1016/j.jprot.2012.03.010

reactive oxygen species (ROS) has been reported to be an important factor in berberine-induced apoptosis of cancer cells [9]. However, the detailed mechanisms of berberine-induced cytotoxicity remain poorly understood.

Proteomics is a powerful tool to monitor protein expression changes in response to drug treatment. 2-DE remains an important technique in proteomics for global protein profiling within biological samples and plays a complementary role to LC-MS-based analysis [11]. However, reliable quantitative comparison between gels remains the primary challenge in 2-DE analysis. A significant improvement in gel-based protein detection and quantification was achieved by the introduction of 2D-DIGE, where several samples can be co-detected on the same gel using differential fluorescent labeling. This approach alleviates gel-to-gel variation and allows comparison of the relative amount of resolved proteins across different gels using a fluorescently-labeled internal standard. Moreover, the 2D-DIGE technique has the advantages of a broader dynamic range of detection, higher sensitivity and greater reproducibility than traditional 2-DE [11]. This innovative technology relies on the pre-labeling of protein samples on the amino group of lysine residues with fluorescent dyes (Cy2, Cy3 and Cy5) before electrophoresis. Each dye has a distinct fluorescent wavelength, allowing pairs of experimental samples and an internal standard to be simultaneously separated in the same gel. The internal standard, which is a pool of an equal amount of all samples, helps to provide accurate normalization and spot matching and increases statistical confidence in relative quantification across gels [12–14]. More recently, a cysteine labeling version of 2D-DIGE was developed, using ICy dyes (iodoacetyl cyanine dyes) which react with the free thiol group of cysteines via alkylation. The pair of ICy dyes (ICy3 and ICy5) has been used to monitor redox-dependent protein thiol modifications in a model cell system exposed to hydrogen peroxide and in plasma fractions exposed to UVC [15].

The aim of the current study was to use a proteomic approach combining lysine and cysteine 2D-DIGE and MS to investigate the inhibitory effects of berberine on breast cancer cells. MCF-7 cells, originally derived from a pleural effusion of a patient with invasive breast ductal carcinoma, were used as a model system to clarify the molecular effects of berberine including the investigation of berberine-induced redox modification of intracellular proteins.

2. Materials and methods

2.1. Chemicals and reagents

Generic chemicals including berberine and N-acetylcysteine were purchased from Sigma-Aldrich (St. Louis, USA), while reagents for 2D-DIGE were purchased from GE Healthcare (Uppsala, Sweden). The synthesis of the ICy3 and ICy5 dyes has been previously reported by our group. All primary antibodies were purchased from Abcam (Cambridge, UK) andanti-mouse, and anti-rabbit secondary antibodies were purchased from GE Healthcare (Uppsala, Sweden). All the chemicals and biochemicals used in this study were of analytical grade.

2.2. Cell lines and cell cultures

The breast cancer cell line MCF-7 was purchased from the American Type Culture Collection (Manassas, VA) and was maintained in Dulbecco's Modified Eagle's medium (DMEM) supplemented with 10% (v/v) fetal calf serum (FCS), L-glutamine (2 mM), streptomycin (100 μg/mL), and penicillin (100 IU/mL) (all from Gibco-Invitrogen Corp., UK). All cells were incubated at 37 °C and 5% CO_2.

2.3. Sample preparation for proteomic analysis

MCF-7 cells treated with varying concentrations of berberine in complete cell culture medium for 24 h or treated with vehicle (methanol, 0.02% (w/v) in media), were washed twice in 0.5× PBS, drained well and lysed in 2-D lysis buffer containing 4% w/v CHAPS, 7 M urea, 2 M thiourea, 10 mM Tris–HCl pH 8.3 and 1 mM EDTA. Samples were homogenized by passage through a 26-gauge needle 10 times and insoluble material was removed by centrifugation at 13,000 rpm for 30 min at 4 °C. Protein concentrations were determined using the Coomassie Protein Assay Reagent (BioRad).

2.4. Immunoblotting

Immunoblotting was used to verify differential expression of MS-identified proteins. Cells were lysed in a buffer containing 50 mM HEPES pH 7.4, 150 mM NaCl, 1% NP40, 1 mM EDTA, 2 mM sodium orthovanadate, 100 μg/mL AEBSF, 17 μg/mL aprotinin, 1 μg/mL leupeptin, 1 μg/mL pepstatin, 5 μM fenvalerate, 5 μM BpVphen and 1 μM okadaic acid prior to protein quantification using Coomassie Protein Assay Reagent (BioRad). 30 μg of protein sample was diluted in Laemmli sample buffer (final concentrations: 50 mM Tris pH 6.8, 10% (v/v) glycerol, 2% SDS (w/v), 0.01% (w/v) bromophenol blue) and separated by 1D-SDS-PAGE following standard procedures. After electroblotting separated proteins onto 0.45 μm Immobilon P membranes (Millipore), the membranes were blocked with 5% w/v skimmed milk in TBS-T (50 mM Tris pH 8.0, 150 mM NaCl and 0.1% Tween-20 (v/v)) for 1 h. Membranes were then incubated in primary antibody solution in TBS-T containing 0.02% (w/v) sodium azide for 2 h. Membranes were washed in TBS-T (3×10 min) and then probed with the appropriate horseradish peroxidase-coupled secondary antibody (GE Healthcare). After further washing with TBS-T, immunoprobed proteins were visualized using an enhanced chemiluminescence method (Visual Protein Co.).

2.5. MTT cell viability assay

MCF-7 cells growing exponentially were trypsinized, counted using a hemocytometer and 10,000 cells/well were seeded into 96-well plates. The culture was then incubated for 24 h before pre-treatment with the indicated concentrations of berberine for 24 h or left untreated. After removal of the medium, 50 μL of MTT working solution (1 mg/mL) (Sigma) was added to the cells in each well, followed by a further incubation at 37 °C for 4 h. The supernatant was carefully removed. 100 μL of DMSO was added to each well and the plates were shaken for 20 min. The absorbance of samples was then

measured at 540 nm in a multi-well plate reader. Values were normalized against the untreated samples and were averaged from 4 independent measurements.

2.6. Assay for endogenous reactive oxygen species using DCFH-DA

MCF-7 cells (10,000 cells/well) were incubated with the indicated concentrations of berberine for 20 min. After two washes with PBS, cells were treated with 10 μM of 2,7-dichlorofluorescin diacetate (DCFH-DA; Molecular Probes) at 37 °C for 20 min, and subsequently washed with PBS. Fluorescence was recorded at an excitation wavelength of 485 nm and emission wavelength of 530 nm.

2.7. Assay for the effect of N-acetylcysteine on berberine-induced cell death

To examine the effect of an antioxidant, N-acetylcysteine (NAC), on berberine-induced cell death, cells were pretreated with NAC (10 and 20 mM) or vehicle (PBS) for 3 h before the treatment with indicated concentrations of berberine (0, 50 and 100 μg/ml) for 20 min or left untreated. After removal of the medium, 50 μL of MTT working solution (1 mg/mL) (Sigma) was added to the cells in each well, followed by a further incubation at 37 °C for 4 h. The supernatant was carefully removed. 100 μL of DMSO was added to each well and the plates were shaken for 20 min. The absorbance of samples was then measured at 540 nm in a multi-well plate reader. Values were normalized against the untreated samples and were averaged from 4 independent measurements.

2.8. 2D-DIGE and gel image analysis

For expression 2D-DIGE, protein samples were labeled with cyanine dyes Cy2, Cy3 and Cy5 according to our previous report [16]. Briefly, 100 μg of protein sample in triplicate was minimally labeled with 250 pmol of either Cy3 or Cy5 for comparison on the same 2-DE gel. To facilitate image matching and cross-gel statistical comparison, a pool of all samples was also prepared and labeled with Cy2 at a molar ratio of 2.5 pmol Cy2 per μg of protein as an internal standard run on all gels. The labeling reactions were performed for 30 min on ice in the dark and then quenched with a 20-fold molar excess of free L-lysine to dye for 10 min. The differentially Cy3- and Cy5-labeled samples were then mixed with the Cy2-labeled internal standard and reduced with dithiothreitol for 10 min. IPG buffer, pH3-10 nonlinear (2% (v/v), GE Healthcare) was added and the final volume was adjusted to 450 μL with 2D-lysis buffer for overnight rehydration into immobilized non-linear pH gradient (IPG) strips (pH 3–10, 24 cm). Isoelectric focusing was then performed using a Multiphor II apparatus (GE Healthcare) for a total of 62.5 kVh at 20 °C. Strips were then equilibrated in 6 M urea, 30% (v/v) glycerol, 1% SDS (w/v), 100 mM Tris–HCl (pH 8.8) with 65 mM dithiothreitol for 15 min and then in the same buffer containing 240 mM iodoacetamide for a further 15 min. Equilibrated IPG strips were transferred onto 24×20 cm 12.5% polyacrylamide gels cast between low-fluorescence glass plates and bonded to one of the plates. The strips were overlaid with 0.5% (w/v) low melting point agarose in running buffer containing bromophenol blue. The gels were run in an Ettan Twelve gel tank (GE Healthcare) at 4 W per gel at 10 °C until the dye front had completely run off the bottom of the gels. Gels were then scanned directly between the glass plates using an Ettan DIGE Imager (GE Healthcare) according to the manufacturer's instructions. Image analysis was performed using DeCyder 2-D Differential Analysis Software v7.0 (GE Healthcare) to co-detect, normalize and quantify the protein features in the images. Features detected from non-protein sources were filtered out. Spots displaying a $\geq$1.5 average-fold increase or decrease in abundance with a P value $<$0.05 were selected for protein identification.

For redox DIGE analysis, cells were lysed in 2-DE buffer (4% w/v CHAPS, 8 M urea, 10 mM Tris–HCl pH 8.3 and 1 mM EDTA) in the presence of ICy3 or ICy5 (80 pmol/mg protein) on ice to limit post-lysis thiol modification. Test samples were labeled with the ICy5 dye and mixed with an equal amount of a standard pool of both samples labeled with ICy3. Since ICy dyes interfered with the protein assay, protein concentrations were determined on replica lysates not containing dye. Lysates were left in the dark for 1 h followed by labeling with Cy2 to monitor protein level. The reactions were quenched with DTT (65 mM final concentration) for 10 min followed by L-lysine (20-fold molar ratio excess of free L-lysine to Cy2 dye) for a further 10 min. Volumes were adjusted to 450 μL with buffer plus DTT and IPG buffer for rehydration. All samples were run in triplicate against the standard pool.

2.9. Protein staining

Colloidal Coomassie Blue G-250 staining was used to visualize CyDye-labeled protein features in 2-DE. Bonded gels were fixed in 30% v/v ethanol, 2% v/v phosphoric acid overnight, washed three times (30 min each) with ddH_2O and then incubated in 34% v/v methanol, 17% w/v ammonium sulfate, and 3% v/v phosphoric acid for 1 h prior to adding 0.5 g/L Coomassie Blue G-250. The gels were then left to stain for 5–7 days. The stained gels were then imaged on an ImageScanner III densitometer (GE Healthcare).

2.10. In-gel digestion

Excised post-stained gel pieces were washed three times in 50% acetonitrile (ACN), dried in a SpeedVac for 20 min, reduced with 10 mM dithiothreitol in 5 mM ammonium bicarbonate pH 8.0 (AmBic) for 45 min at 50 °C and then alkylated with 50 mM iodoacetamide in 5 mM AmBic for 1 h at room temperature in the dark. The gel pieces were then washed three times in 50% ACN and vacuum-dried before reswelling with 50 ng of modified trypsin (Promega) in 5 mM AmBic. The pieces were then overlaid with 10 μL of 5 mM AmBic and trypsinized for 16 h at 37 °C. Supernatants were collected, peptides were further extracted twice with 5% trifluoroacetic acid (TFA) in 50% ACN and the supernatants were pooled. Peptide extracts were vacuum-dried, resuspended in 5 μL ddH_2O, and stored at −20 °C prior to MS analysis.

2.11. Protein identification by MALDI-TOF MS and MS/MS

For protein identification, extracted peptides were subjected to peptide mass fingerprinting (PMF) using MALDI-TOF MS. Briefly, 0.5 μL of trypsin digested protein sample was

mixed with 0.5 μL of a matrix solution containing α-cyano-4-hydroxycinammic acid at a concentration of 1 mg/mL of 50% ACN/0.1% TFA (v/v), spotted onto an anchorchip target plate (Bruker Daltonics) and dried. The peptide mass fingerprints were acquired using an Autoflex III mass spectrometer (Bruker Daltonics) in reflector mode. The algorithm used for spectral annotation was SNAP (Sophisticated Numerical Annotation Procedure). The following metrics were used: Peak detection algorithm: SNAP; Signal to noise threshold: 25; Relative intensity threshold: 0%; Minimum intensity threshold: 0; Maximal number of peaks: 50; Quality factor threshold: 1000; SNAP average composition: Averaging; Baseline subtraction: Median; Flatness: 0.8; Median level: 0.5. The spectrometer was also calibrated with a peptide calibration standard (Bruker Daltonics) and internal calibration was performed using trypsin autolysis peaks at *m/z* 842.51 and *m/z* 2211.10. Peaks in the mass range of *m/z* 800–3000 were used to generate a peptide mass fingerprint that was searched against the Swiss-Prot/TrEMBL database (v57.12; 513,877 entries) using Mascot software v2.2.06 (Matrix Science, London, UK). The following parameters were used: *Homo sapiens*; tryptic digest with a maximum of 1 missed cleavage; carbamidomethylation of cysteine, partial protein N-terminal acetylation, partial methionine oxidation, partial modification of glutamine to pyroglutamate, ICy3 (C34 H44 N3 O) and ICy5 (C34 H42 N3 O) and a mass tolerance of 50 ppm. Identifications were accepted based on significant MASCOT scores ($P<0.05$), at least 4 peptides per protein, spectral annotation and observed versus expected molecular weight and pI on 2-DE. MALDI-TOF/TOF analysis was performed on the same instrument using the LIFT mode. MS/MS ion searches were performed using Mascot with the same search parameters as above and using an MS/MS tolerance of ±0.2 Da.

2.12. *Enzyme-linked immunosorbent assay (ELISA) analysis*

EIA polystyrene microtiter plates were coated with 50 μg of protein lysate sample and incubated at 37 °C for 2 h. The

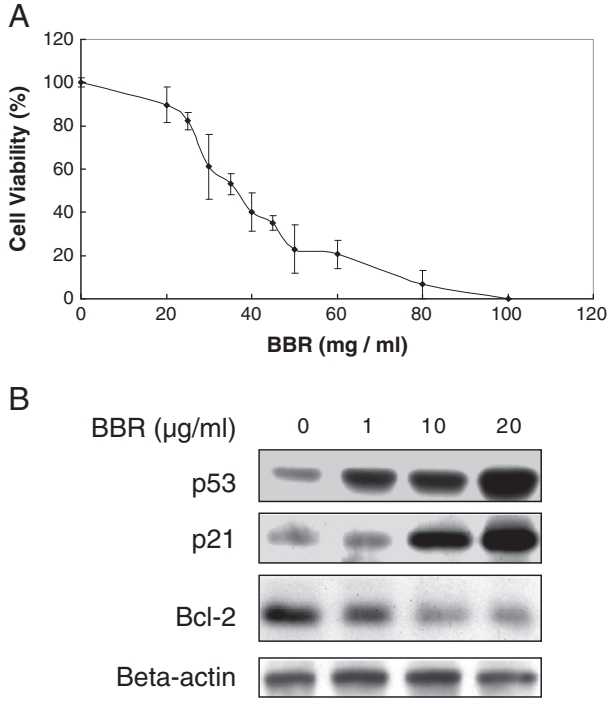

Fig. 1 – Berberine-induced loss of cell viability and analysis of cell cycle and cell survival regulator expression. (A) MTT-based viability assays were performed where 10,000 MCF-7 cells were plated into 96-well plates in medium containing 10% FBS. After 24 h, the cells were treated with the indicated concentrations of berberine for a further 24 h. Cells were incubated with MTT and then DMSO was added and the plates were shaken for 20 min followed by measurement of the absorbance at 540 nm. Values were normalized against untreated samples and are the average of 4 independent measurements +/– the standard deviation. (B) Activation of apoptosis, cell cycle inhibition and survival signaling pathways were analyzed by immunoblotting with anti-p53, anti-p21 and anti-Bcl2 antibodies, respectively.

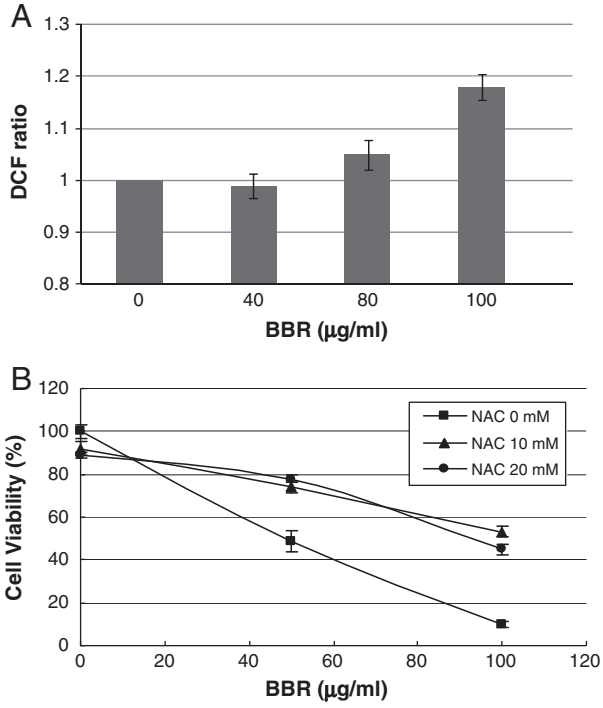

Fig. 2 – Effect of berberine on MCF-7 ROS production. (A) DCFH-based intracellular ROS production assays were performed where 100,000 MCF-7 cells were plated into 24-well plates in medium containing 10% FBS. After 24 h, the cells were treated with the indicated concentrations of berberine for a further 20 min. Cells were then treated with 10 μM of DCFH-DA at 37 °C for 20 min and the fluorescence was recorded at excitation and emission wavelengths of 485 nm and 530 nm, respectively. (B) Pretreatment of NAC (10 mM and 20 mM) or vehicle (PBS) inhibits berberine-induced cell death in MCF-7 cells. Cells were treated with varying concentrations of berberine (0, 50 and 100 μg/ml) for 24 h then harvested for analysis of cell viability using the MTT assay as detailed in Materials and methods.

plate was washed three times with phosphate buffered saline with Tween-20 (PBS-T) and three times with PBS. Plates were then blocked with 100 μL of 5% skimmed milk in PBS at 37 °C for 2 h and then washed three times with PBST. Antibody (Abcam) solution was added and incubated at 37 °C for 2 h. After washing with PBST and PBS for 10 times in total, 100 μL of peroxidase-conjugated secondary antibody in PBS was added for incubation at 37 °C for 2 h. Following 10 washes, 100 μL of 3,3′,5,5′-tetramethyl benzidine (Pierce) was added. After incubation at room temperature for 30 min, 100 μL of 1 M H_2SO_4 was added to stop the reaction and the absorbance at 450 nm was measured using a Stat Fax 2100 microtiter plate reader (Awareness Technology Inc. FL, USA).

2.13. *Validation of thiol reactivity changes by immunoprecipitation coupled to immunoblotting*

Berberine treated MCF-7 cells were lysed in the presence of ICy3 or ICy5 dyes to limit post-lysis thiol modification. The labeling reactions were performed in the dark at 37 °C for 1 h and then quenched with a 2-fold molar excess of DTT for 10 min. 500 μg of ICy dye-labeled cell lysate was then diluted

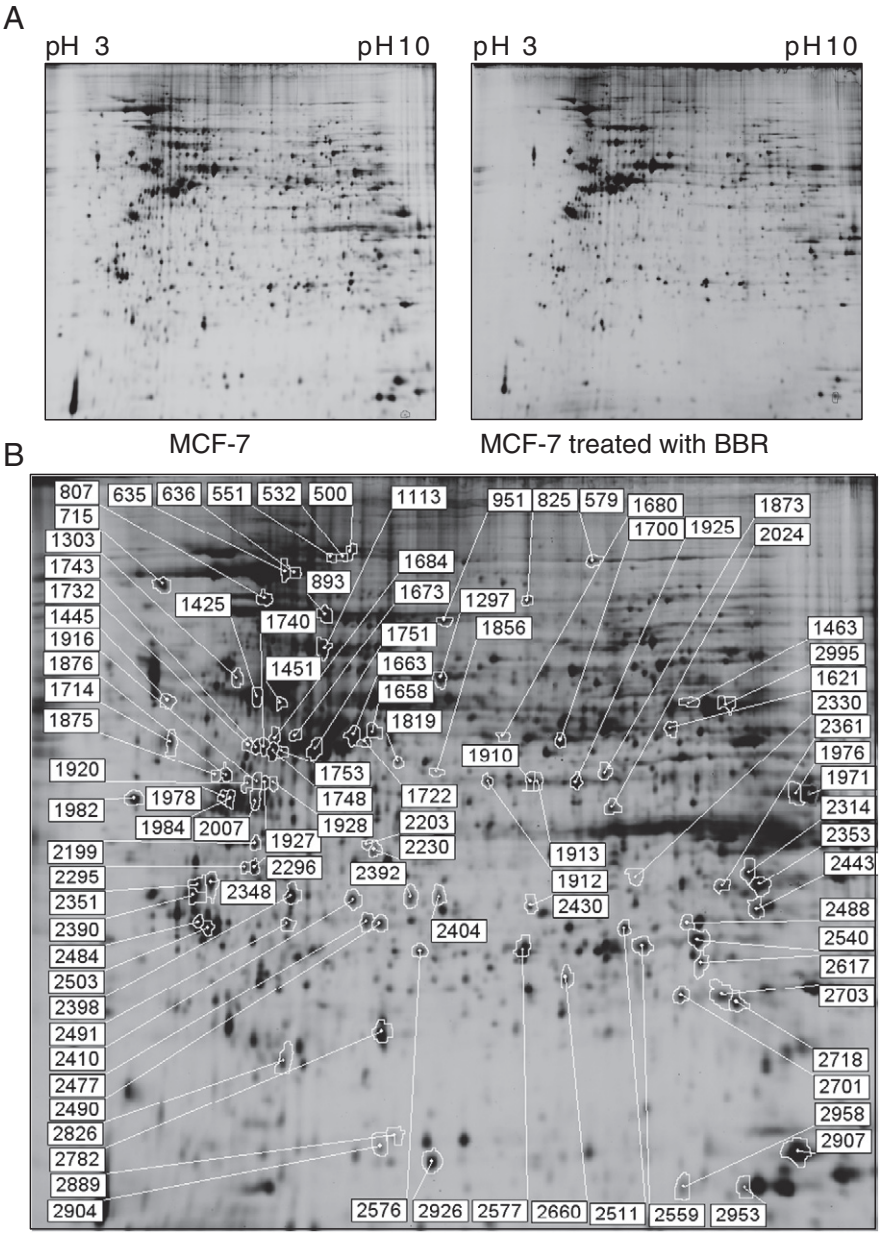

Fig. 3 – 2D-DIGE analysis of berberine-induced differential protein expression in MCF-7 cells. (A) MCF-7 cells were treated with an IC_{50} concentration of berberine for 24 h or left untreated. Lysates were prepared in triplicate and 2D-DIGE analysis was performed according to Materials and methods. 2D-DIGE images of the protein samples from untreated and berberine-treated MCF-7 cells are displayed, respectively. (B) Differentially expressed protein features are annotated with spot numbers.

Table 1 – List of berberine-induced differentially expressed MCF-7 proteins identified by MALDI-TOF peptide mass fingerprinting after 2D-DIGE analysis.

No.	Accession no.	Protein name	pI	MW	Match. peptides	Cov. (%)	Score	MCF7-ber/ MCF7	t-Test	Matched peptide sequences	Subcellular location	Function classification
2889	Q9BV57	1,2-Dihydroxy-3-keto-5-methylthiopentene dioxygenase	5.43	21,542	5/9	29	58/56	−2.66	0.0011	R.QPHRPDPGRPVGLEQLR.R; R.YILDGSGYFDVR.D	Cytoplasm	Metabolism
2503	P63104	14-3-3 Protein zeta/delta	4.73	27,899	10/23	36	100/56	−4.21	2.50E−06	K.GIVDQSQQAYQEAFEISK.K; K.KEMQPTHPIR.L	Cytoplasm	Cell signaling
1819	Q9UNM6	26S proteasome non-ATPase regulatory subunit 13	5.53	43,176	6/15	21	58/56	−1.65	0.0045	R.VNPLSLVEIILHVVR.Q;K.LYENFISEFEHR.V	Cytoplasm	Proteolysis
1876	P08865	40S ribosomal protein SA	4.79	32,947	5/15	32	59/56	−3.22	1.20E−05	K.FAAATGATPIAGR.F; R.FTPGTFTNQIQAAFR.E	Cytoplasm	Protein synthesis
807	P11021	78 kDa glucose-regulated protein (GRP-78)	5.07	72,402	9/29	17	75/56	2.22	0.0094	R.IEIESFYEGEDFSETLTR.A; K.SDIDEIVLVGGSTR.I	ER	Protein folding
1113	P60709	Actin, cytoplasmic 1	5.29	42,052	10/31	35	100/56	1.64	0.0068	K.DLYANTVLSGGTTMYPGIADR.M; R.VAPEEHPV LLTEAPLNPK.A	Cytoplasm	Cytoskeleton
1714	P05141	ADP/ATP translocase 2/Adenine nucleotide translocase-2/ANT2	9.76	33,102	5/8	20	58/56	1.71	0.0003	K.EQGVLSFWR.G;- .MTDAAVSFAKDFLAGGVAAAISK.T	Mitochondrion	Transport
1463	Q9H0F7	ADP-ribosylation factor-like protein 6	8.72	21,255	5/13	29	70/56	−2.27	0.0077	R.QLVNMCINPDPEK.R;K.RPDVTYVYDVAK.R	Cytoplasm	Cell signaling
532	O43707	Alpha-actinin-4	5.27	105,245	10/26	12	70/56	−1.71	0.0031	K.TFTAWCNSHLR.K;K.DGLAFNALIHR.H	Cytoplasm	Cytoskeleton
1971	P06733	Alpha-enolase	7.01	47,481	6/13	15	57/56	−5.96	2.40E−05	K.LAMQEFMILPVGAANFR.E; R.YISPDQLADLYK.S	Cytoplasm	Metabolism
2995	P06733	Alpha-enolase	7.01	47,481	10/24	22	71/56	−4.62	0.0016	K.LAQANGWGVMVSHR.S; R.AAVPSGASTGIYEAL ELR.D	Cytoplasm	Metabolism
2296	P08758	Annexin A5	4.94	35,971	9/21	35	108/56	−3.04	0.00069	K.GLGTDEESILTLLTSR.S;R.LYDAYELK.H	Membrane	Cell signaling
2295	P08758	Annexin A5	4.94	35,971	6/17	20	65/56	−2.04	0.0014	R.MLVVLLQANR.D;K.VLTEIIASR.T	Membrane	Cell signaling
1425	P06576	ATP synthase subunit beta, mitochondrial	5.26	56,525	10/31	28	91/56	−1.61	0.00099	R.IMDPNIVGSEHYDVAR.G; R.FLSQPFQVAEVFTG HMGK.L	Mitochondrion	Electron transport
1451	Q8IYB8	ATP-dependent RNA helicase SUPV3L1, mitochondrial	8.2	88,791	5/8	10	58/56	2.13	0.00018	R.FMDMFPDASLIRDLQK.E; K.EGEVTTMNHEDLSL LKEILK.R	Mitochondrion	Gene regulation
1297	Q9BV35	Calcium-binding mitochondrial carrier protein SCaMC-3	6.85	52,573	7/21	19	66/56	2.43	0.00015	R.GIAPNFMKVIPAVSISYVVYENMK.Q; K.QLVAGA VAGAVSR.T	Mitochondrion	Calcium transport
1673	Q9BV35	Calcium-binding mitochondrial carrier protein SCaMC-3	6.85	52,573	7/20	19	68/56	2.44	0.0021	K.QLVAGAVAGAVSR.T; R.GIAPNFMKVIPAVSISY VVYENMK.Q	Mitochondrion	Calcium Transport
579	P19784	Casein kinase II subunit alpha	8.65	41,358	5/7	18	59/56	−2.15	0.0024	K.GIMHRDVKPHNVMIDHQQK.K; R.LIDWGLAEFY HPAQEYNVR.V	Nucleus	Cell signaling
1875	Q9H9A5	CCR4-NOT transcription complex subunit 10	7.95	83,398	5/9	11	57/56	−1.58	0.017	R.TVMLFNLGSAYCLRSEYDK.A; K.CLHQAASMIH PK.E	Nucleus	Gene regulation
2390	P10747	CD28	9.46	25,392	6/15	28	67/56	−3.73	2.20E−05	K.YSYNLFSREFR.A;R.LLHSDYMNMTPR.R	Membrane	Immunoregulation
2398	O00299	Chloride intracellular channel protein 1/CLIC1/NCC27	5.09	27,248	7/14	26	99/56	−2.31	0.00029	K.IGNCPFSQR.L;M.AEEQPQVELFVK.A	Nucleus	Redox-regulation
1910	Q86WR0	Coiled-coil domain-containing protein 25	6.34	24,634	5/13	22	61/56	−2.03	0.00017	K.DKYENEDLIK.H;K.LSSAHVYLR.L	Nucleus	Gene regulation
500	Q9H2F9	Coiled-coil domain-containing protein 68	8.78	39,073	6/16	17	59/56	−1.76	0.011	K.QLLQVNK.L;R.NVAQRLFENYQTQSEEVR.K	Nucleus	Gene regulation
1976	P0C862	Complement C1q tumor necrosis factor-related protein 9A	8.59	34,831	5/16	24	57/56	−5.03	7.50E−05	R.GSPGKHGPK.G; K.GDKGDAGEPGRPGSPGK.D	Secreted	Cell signaling
1982	Q9P2B4	CTTNBP2 N-terminal-like protein	8.22	70,571	7/20	21	60/56	−2.88	0.00023	K.THSQAASLTTAEDLASSCSSNTVVANGK.D; R.HA QDTAEGDDVTYMLEKER.E	Unknown	Unknown
2430	Q8WUJ1	Cytochrome b5 domain-containing protein 2	8.73	29,184	5/10	24	57/56	−1.57	0.014	R.LMGWWGPRAGFR.L; R.FYGEDGLPTPALTQVEA AITR.G	ER	Detoxification

(continued on next page)

Table 1 *(continued)*

No.	Accession no.	Protein name	pI	MW	Match. peptides	Cov. (%)	Score	MCF7-ber/ MCF7	t-Test	Matched peptide sequences	Subcellular location	Function classification
2203	P52907	F-actin-capping protein subunit alpha-1	5.45	33,073	5/12	26	68/56	−1.56	0.002	R.LLLNNDNLLR.E; K.IEGYEDQVLITEHGDLGNSR. F	Cytoplasm	Cytoskeleton
2348	P04075	Fructose-bisphosphate aldolase A	8.3	39,851	6/17	28	71/56	−3.14	0.00048	K.CPLLKPWALTFSYGR.A; K.IGEHTPSALAIMENA NVLAR.Y	Cytoplasm	Metabolism
2199	A6NC05	Glutaredoxin-like protein YDR286C homolog	8.49	13,552	4/14	34	58/56	−2.58	5.00E−05	K.TTLPVLTLFTK.D;K.TTLPVLTLFTK.D	Cytoplasm	Electron transport
951	O00461	Golgi integral membrane protein 4	4.73	81,888	6/13	13	57/56	1.53	0.0041	R.YSALNVQHQMLKSQHEELK.K; R.YSALNVQHQ MLKSQHEELK.K	Golgi	Protein trafficking
1751	Q8IUY3	GRAM domain-containing protein 2	8.73	40,908	5/11	14	57/5	−1.57	0.0002	.MTALSR.S;R.RVCTHLQPSSK.K	Membrane	Unknown
2703	P62826	GTP-binding nuclear protein Ran	7.01	24,579	6/16	36	79/56	−1.77	0.0015	K.NLQYYDISAK.S;K.SNYNFEKPFLWLAR.K	Nucleus	Protein trafficking
2353	P63244	Guanine nucleotide-binding protein subunit beta-2-like 1	7.6	35,511	7/14	32	96/56	−2.03	0.00014	K.HLYTLDGGDIINALCFSPNR.Y; R.VWQVTIGTR.-	Membrane	Cell signaling
893	P11142	Heat shock cognate 71 kDa protein	5.37	71,082	8/18	16	76/56	−1.92	1.40E−06	K.TVTNAVVTVPAYFNDSQR.Q; R.FEELNADLFR.G	Cytoplasm	Protein folding
2576	Q9UC36	Heat shock protein beta-1/ HSP-27	5.98	22,826	9/56	40	81/56	1.96	6.40E−05	K.LATQSNEITIPVTFESR.A;R.QLSSGVSEIR.H	Cytoplasm	Protein folding
2577	P04792	Heat shock protein beta-1/ HSP-27	5.98	22,826	9/30	40	94/56	2.04	0.0032	K.LATQSNEITIPVTFESR.A;R.QLSSGVSEIR.H	Cytoplasm	Protein folding
636	P08238	Heat shock protein HSP 90-beta	4.97	83,554	10/22	16	75/56	−1.65	0.01	R.ALLFIPR.R; K.HNDDEQYAWESSAGGSFTVR.A	Cytoplasm	Protein folding
2024	P31942	Heterogeneous nuclear ribonucleoprotein H3(hnRNP H3)	6.37	36,960	7/21	35	75/56	−2.26	0.00035	R.GMGGHGYGGAGDASSGFHGGHFVHMR.G; R.ATENDIANFFSPLNPIR.V	Nucleus	Gene regulation
1928	P07910	Heterogeneous nuclear ribonucleoproteins C1/C2 (hnRNP C1/ hnRNP C2)	4.95	33,707	6/12	19	66/56	2.21	0.0022	K.GFAFVQYVNER.N;R.VPPPPPIAR.A	Nucleus	Gene regulation
1920	P07910	Heterogeneous nuclear ribonucleoproteins C1/C2(hnRNP C1/ hnRNP C2)	4.95	33,707	5/9	16	58/56	2.02	5.60E−04	R.VPPPPPIAR.A;K.SGFNSKSGQR.G	Nucleus	Gene regulation
1927	P07910	Heterogeneous nuclear ribonucleoproteins C1/C2(hnRNP C1/ hnRNP C2)	4.95	33,707	5/9	15	56/56	1.89	0.0022	K.SDVEAIFSKYGK.I;R.VPPPPPIAR.A	Nucleus	Gene regulation
1916	P07910	Heterogeneous nuclear ribonucleoproteins C1/C2(hnRNP C1/hnRNP C2)	4.95	33,707	5/10	16	57/56	1.72	5.90E−03	K.SDVEAIFSKYGK.I;K.GFAFVQYVNER.N	Nucleus	Nucleus regulation
1722	Q13547	Histone deacetylase 1/HDAC1	5.31	55,638	8/14	23	84/56	1.72	0.0022	K.YHSDDYIKFLR.S: K.SFNLPMLMLGGGGYTIRNVAR.C	Nucleus	Gene regulation
2491	Q96JB3	Hypermethylated in cancer 2 protein	5.95	67,140	6/18	11	64/56	−2.93	7.70E−05	R.LSTASVIQAR.Y;K.EEEENGK.D	Nucleus	Gene regulation
2484	O14879	Interferon-induced protein with tetratricopeptide repeats 3 (IFIT-3)	5.12	56,691	5/11	13	58/56	−3.14	1.70E−05	K.KFSNPYSIEYSELDCEEGWTQLK.C; K.QYAMDYSNK.A	Membrane	Cell signaling
2904	Q9H095	IQ domain-containing protein G	6.18	51,999	5/8	12	58/56	1.53	0.029	K.MHFYDIIAREEK.G;K.SREMNLEGTNLDK.L	Unknown	Unknown
1663	P05783	Keratin, type I cytoskeletal 18	5.34	48,029	9/15	18	89/56	1.92	9.50E−05	K.VKLEAEIATYR.R;K.EELLFMKK.N	Cytoplasm	Cytoskeleton
1740	P08727	Keratin, type I cytoskeletal 19	5.04	44,065	9/28	24	85/56	2.19	4.20E−05	K.IRDWYQK.Q;R.IVLQIDNAR.L	Cytoplasm	Cytoskeleton
1743	P08727	Keratin, type I cytoskeletal 19	5.04	44,065	18/36	40	180/56	3.47	5.00E−05	R.LASYLDKVR.A;R.KDAEAWFTSR.T	Cytoplasm	Cytoskeleton
1732	P08727	Keratin, type I cytoskeletal 19	5.04	44,065	5/12	15	57/56	2.38	0.00041	R.FGPGVAFR.A; R.FGAQLAHIQALISGIEAQLGDVRA	Cytoplasm	Cytoskeleton
1753	P08727	Keratin, type I cytoskeletal 19	5.04	44,065	10/23	25	103/56	1.94	0.0019	R.QSSATSSFGGLGGGSVR.F;R.FGPGVAFR.A	Cytoplasm	Cytoskeleton
2617	P04264	Keratin, type II cytoskeletal 1	5.04	66,149	9/23	25	92/56	−2	0.0022	K.YEELQITAGR.H; R.MSGECAPNVSVSVSTSHTTISGGGSR.G	Cytoplasm	Cytoskeleton
2958	O15229	Kynurenine 3-monooxygenase	5.04	56,344	9/22	25	73/56	−1.95	0.016	R.NTFMMIALPNMNK.S; R.AHVNSSWFIFQKNMER.F	Mitochondrion	Metabolism
2660	P0C5W0	Paraneoplastic antigen-like protein 6B	5.04	44,378	6/9	18	58/56	−2.89	0.0049	R.LEVLLQK.A;- .MAVTMLQDWCRWMGVNAR.R	Cytoplasm	Unknown

2361	P0C5W0	Paraneoplastic antigen-like protein 6B	5.04	44,378	6/13	20	59/56	−2.03	0.0072	K.EALARASADR.V;R.LEVLLQK.A	Cytoplasm	Unknown
2953	P62937	Peptidyl-prolyl cis-trans isomerase A (PPIase A/Cyclophilin A)	5.04	18,229	6/17	46	57/56	−2.23	0.022	R.IIPGFMCQGGDFTR.H;K.FEDENFILK.H	Cytoplasm	Protein folding
2782	P32119	Peroxiredoxin-2	5.04	22,049	6/21	34	82/56	−5.02	5.60E−06	R.KEGGLGPLNIPLLADVTR.R; K.EGGLGPLNIPLLADVTR.R	Cytoplasm	Redox-regulation
2477	Q13162	Peroxiredoxin-4 (Prx-IV)	5.86	30,749	6/18	29	61/56	1.72	0.004	0.004	Cytoplasm	Redox-regulation
2511	P30041	Peroxiredoxin-6	5.04	25,133	9/31	43	101/56	−3.12	0.00072	R.FHDFLGDSWGILFSHPR.D; M.PGGLLLGDVAPNFEANTTVGR.I	Cytoplasm	Redox-regulation
715	Q15124	Phosphoglucomutase-like protein 5/PGM-RP	5.04	62,756	6/12	14	67/56	1.69	0.0024	R.LGRQEFDLENK.F;R.SMPTSMALDR.V	Cytoplasm	Cytoskeleton
1912	Q96DM1	PiggyBac transposable element-derived protein 4	5.04	67,702	6/15	12	57/56	−1.81	0.0042	K.EVTMLSTFHNDTVIEVNNR.N; R.YFCAECDVPLCVVPCFEIYHTK.K	Unknown	Unknown
2701	Q9Y646	Plasma glutamate carboxypeptidase	5.04	52,083	5/16	19	58/56	−2.41	0.00086	R.LALLVDTVGPRLSGSK.N; M.KFLIFAFFGGVHLLSLCSGK.A	Secreted	Proteolysis
2718	Q9UHX1	Poly(U)-binding-splicing factor PUF60	5.04	60,009	5/12	16	57/56	−1.7	0.018	K.AQSSQDAVSSMNLFDLGGQYLRVGK.A; K.QESTVMVLR.N	Nucleus	Gene regulation
1684	Q9BY77	Polymerase delta-interacting protein 3/p46/S6K1 Aly/REF-like target/SKAR/POLDIP3	5.04	46,289	5/12	19	57/56	1.78	0.0027	K.CNLHMNGNVITSDQPILLR.L; K.QNLYDLDEDDDGIASVPTK.Q	GIASVPTK.Q	Protein synthesis
2490	P35232	Prohibitin	5.04	29,843	11/37	51	110/56	2.93	1.00E−05	R.IFTSIGEDYDER.V; K.FGLALAVAGGVVNSALYNVDAGHR.A	Mitochondrion	Anti-proliferation
1748	O14511	Pro-neuregulin-2/ Pro-NRG2	5.04	93,104	5/8	9	58/56	2.16	0.00011	K.NVPATDHVIR.R; K.VQGLVPAGGSSSNSTREPPA SGR.V	Membrane	Cell signaling
2410	Q9UL46	Proteasome activator complex subunit 2	5.04	27,515	5/8	29	61/56	61/56	5.00E−06	R.QNLFQEAEEFLYR.F; K.IIYLNQLLQEDSLNVADL TSLR.A	Cytoplasm	Proteolysis
2351	P61289	Proteasome activator complex subunit 3	5.04	29,602	6/16	26	70/56	−3.12	8.20E−06	K.KLLELDSFLK.E;M.ASLLKVDQEVK.L	Cytoplasm	Proteolysis
2404	P61289	Proteasome activator complex subunit 3	5.04	29,602	6/19	22	64/56	−2.43	0.00047	R.TVTEIDEKEYISLR.L;K.LKVDSFR.E	Cytoplasm	Proteolysis
2926	Q5SRD0	Protein FAM21D	5.04	33,352	5/13	21	56/56	−4.57	2.20E−05	R.SAQAAPEPR.F; R.GPIAQWADGAISPNGHRPQLR.A	Unknown	Unknown
1680	Q6IQ22	Putative Ras-related protein Rab-12	5.04	27,573	6/18	19	58/56	1.99	0.0005	R.KQPPRPADFK.L;K.FAQQITGMR.F	Golgi	Protein trafficking
635	Q9BYM8	RanBP-type and C3HC4-type zinc finger-containing protein 1/ RBCK1	5.04	59,359	8/27	19	69/56	−1.84	0.0086	R.GPLEPGPPKPGVPQEPGR.G; R.ARPEAYQVPASYQPDEEERAR.L	Cytoplasm	Proteolysis
1621	Q8WUD1	Ras-related protein Rab-2B	5.04	24,427	5/15	33	64/56	1.6	0.0012	R.SITRSYYR.G;-.MTYAYLFKYIIIGDTGVGK.S	Membrane	Protein trafficking
2826	Q14964	Ras-related protein Rab-39A (Rab-39)	5.04	25,390	4/8	22	58/56	1.93	1.70E−05	R.FPGLRSPACDPTVGVDFFSR.L; R.RSFEHVK.D	Membrane	Protein trafficking
2330	Q96LZ7	Regulator of microtubule dynamics protein 2/RMD-2	5.04	47,711	6/13	18	70/56	2.34	0.021	R.AYGDMYELSTNTQEK.K;K.IMTSLKR.-	Membrane	Unknown
1445	Q14563	Semaphorin-3A	5.04	89,916	5/8	10	59/56	−1.6	0.016	K.VTLEVIDTEHLEELLHKDDDGDGSK.T; R.VPYPRPGTCPSKTFGGFDSTK.D	Secreted	Growth regulation
1856	Q969Q6	Serine/threonine-protein phosphatase 2A regulatory subunit B	5.04	53,567	5/10	15	59/56	8.72	0.015	R.AIQELMKIHGQDPVSFQDVK.D; R.KVWLHQTR.I	Cytoplasm	Cell signaling
1873	P55809	Succinyl-CoA:3-ketoacid-coenzyme A transferase 1, mitochondrial/ OXCT1	5.04	56,578	5/10	5/10	58/56	−1.86	0.001	K.ETVTILPGASFFSSDESFAMIR.G; R.QYLSGELEVELTPQGTLAER.I	Mitochondrion	Metabolism
1658	Q9NYB0	Telomeric repeat-binding factor 2-interacting protein 1/ hRAP1	5.04	44,404	5/11	11	60/56	2.64	0.0012	K.ENARSPSSVTGNALWK.A; R.NERLELEAYR.L	Nucleus	Gene regulation
2488	A6NLP5	Tetratricopeptide repeat protein 36 (TPR repeat protein 36)/ HBP21	5.04	20,998	5/16	41	57/56	−1.59	1.40E−03	R.AARLGSPFAR.R; K.EEREEDEVFPQAQLEQSK.A	Cytoplasm	Protein folding
2443	Q3KNT9	Transmembrane protein 95	5.04	20,154	5/12	26	58/56	−1.59	0.0027	R.LPAHDLSGR.L; R.QKECGASPDFSAFALDEVSMNK.V	Membrane	Unknown

(continued on next page)

Table 1 *(continued)*

No.	Accession no.	Protein name	pI	MW	Match. peptides	Cov. (%)	Score	MCF7-ber/ MCF7	t-Test	Matched peptide sequences	Subcellular location	Function classification
2559	P60174	Triosephosphate isomerase	5.04	26,938	6/15	27	80/56	−2.38	0.0015	R.KFFVGGNWK.M; K.VPADTEVVCAPPTAYIDFAR.Q	Cytoplasm	Metabolism
2540	P60174	Triosephosphate isomerase	5.04	26,938	7/19	43	93/56	−3.57	7.20E−06	K.VPADTEVVCAPPTAYIDFAR.Q; K.FFVGGNWK.M	Cytoplasm	Metabolism
2907	Q9UI30	TRM112-like protein TRM112-like protein	5.04	14,304	5/19	49	62/56	−2.56	0.00028	R.LIQVPKGPVEGYEENEEFLR.T; R.GIPNMLLSEEETES.-	Cytoplasm	Protein synthesis
2230	Q9NV66	tRNA wybutosine-synthesizing protein 1 homolog	5.04	84,732	7/12	8	61/56	1.54	0.0028	K.TQGKNLQEK.S;K.HGSIEADFR.A	Cytoplasm	Protein synthesis
825	Q8NHU6	Tudor domain-containing protein 7	5.04	125,046	6/9	7	56/56	−1.57	0.041	K.VQPLVDMFR.K;-.MLEGDLVSKMLR.A	Cytoplasm	Gene regulation
1913	Q9NVL8	Uncharacterized protein C14orf105	5.04	34,726	5/11	20	58/56	−2.29	4.20E−05	R.QEAQMELKK.S;-.MGLSHSKTHLR.V	Unknown	Unknown
1925	Q9NVL8	Uncharacterized protein C14orf105	5.04	34,726	6/11	23	72/56	−2.21	0.00029	R.QEAQMELKK.S;-.MGLSHSKTHLR.V	Unknown	Unknown
551	Q6ZUT6	Uncharacterized protein C15orf52	5.04	57,803	8/16	15	81//56	−1.75	0.0039	K.NQALLRR.Y;K.KNQALLR.R	Unknown	Unknown
2392	P42696	Uncharacterized protein CXorf22	5.04	48,649	5/12	14	60/56	−2.45	5.50E−05	K.LADRESALASADLEEEIHQK.Q; R.ESALASADLEE EIHQKQGQK.R	Unknown	Unknown
1978	Q96K21	Zinc finger FYVE domain-containing protein 19	5.04	52,411	6/14	20	71/56	2.53	5.40E−06	K.GGGPAASLQNDLNQGGPGSTNSKR.Q; R.CAGCDGDLFCARCFR.E	Nucleus	Gene regulation
1984	Q96K21	Zinc finger FYVE domain-containing protein 19	5.04	52,411	6/14	20	71/56	2.38	4.10E−05	K.DERQGSIPSTQEMEAR.L; K.GGGPAASLQNDLNQGGPGSTNSKR.Q	Nucleus	Gene regulation
1303	Q6ZN57	Zinc finger protein 2 homolog(Zfp-2)	5.04	54,360	5/16	21	57/56	−1.74	0.00099	K.IYECNQCSKTFSQSSSLLK.H; K.CNECGKAFTQSMNLTVHQR.T	Nucleus	Gene regulation
1700	Q8N7K0	Zinc finger protein 433	5.04	79,872	7/16	15	68/56	−2.15	0.00037	K.KWKPQNIYVEYENLR.R; K.KPFNCLSSVQTHERAHSGR.K	Nucleus	Gene regulation
2314	Q96NL3	Zinc finger protein 599	5.04	69,500	5/9	10	57/56	2.45	0.00024	K.AFCDSSSLIQHMR.I; R.IHTGEKPYECSECGK.A	Nucleus	Gene regulation
2007	Q8TD23	Zinc finger protein 675	5.04	68,465	5/7	9	57/56	2.01	0.0076	K.EPLTVKR.H;K.CEECEK.A	Nucleus	Gene regulation

20-fold with NP40 buffer containing protease inhibitors and then incubated with 5 μg primary antibody and 40 μL of a 50% slurry of protein A-Sepharose for 16 h at 4 °C. Immune complexes were then washed three times in lysis buffer and boiled in Laemmli sample buffer prior to resolving by SDS-PAGE. ICy images were scanned directly between low-fluorescence glass plates using an Ettan DIGE Imager (GE Healthcare) followed by immunoblotting analysis with the same primary antibody to detect the specific protein. The immunoblotting procedure is described above.

3. Results

3.1. *Berberine induces cell death in MCF-7 cells*

In our preliminary study, berberine has shown to be less toxic to non-tumorigenic MCF-10A breast cells in comparison to non-invasive breast cancer cells, MCF-7, and invasive breast cancer cells, MDA-MB-231 cell (Supplemental Fig. 1). To evaluate the effect of berberine on breast cancer cells, we exposed MCF-7 cells to a dose range (0–100 μg/mL) of berberine for 24 h and performed MTT assays. Exposure of MCF-7 cells to berberine was shown to result in a dose-dependent loss of cell viability (Fig. 1A). At a berberine concentration of 36.91 μg/mL, a significant loss of cell viability (50%) was detectable after 24 h. In order to verify berberine-induced MCF-7 cell toxicity, we also examine changes in cell survival, apoptosis and cell cycle markers in MCF-7 cells treated with 0–20 μg/mL of berberine for 24 h. The cell survival marker Bcl-2 was down-regulated in a dose-dependent manner, while the apoptotic marker p53 and cell cycle inhibitor p21, were both up-regulated by berberine treatment (Fig. 1B).

3.2. *Berberine induces generation of intracellular ROS in MCF-7 cells*

Previous reports have shown that berberine is able to induce apoptosis in human prostate and colon cancer cells through the generation of ROS [7,9]. However, there is no report of this in breast cancer cells. Accordingly, we tested the hypothesis whether berberine-induced cell death in breast cancer is initiated through ROS generation. Using DCF fluorescence as readout, treatment of MCF-7 cells with berberine for 20 min resulted in a dose-dependent increase in ROS generation compared with untreated MCF-7 cells (Fig. 2A). We further checked whether a cell-permeable anti-oxidant could rescue cells from berberine-induced cell death due to the generation of ROS. The result demonstrated that pretreatment with NAC offered significant protection against berberine-induced cell death in MCF-7 cells at each dose of berberine (Fig. 2B).

3.3. *2D-DIGE and MALDI-TOF MS analysis of berberine-induced proteomic alterations in MCF-7 cells*

In order to analyze berberine-induced proteomic alterations, MCF-7 cells were grown on cell culture dishes prior to treatment with an IC_{50} concentration (36.91 μg/mL) of berberine or treated with vehicle. Three biological replicates for each treatment were compared by 2D-DIGE to provide a global overview of berberine-induced differential protein expression. Image analysis revealed more than 1800 well-defined protein features (Fig. 3A). Those appearing in all replicates and showing a change in average abundance of >1.5-fold ($P<0.05$) between the treated and untreated cell lysates were excised from gels for protein identification. MALDI-TOF MS identification revealed 96 differentially expressed proteins between berberine-treated and untreated MCF-7 cells (Fig. 3B, Supplemental Fig. 2 and Table 1).

Using functional information from the Swiss-Prot and KEGG pathway databases, numerous biological functions were ascribed to the identified proteins with possible roles in berberine-induced cytotoxicity. Fig. 4 compares the expression profiles of the differentially expressed proteins. Proteins known to regulate protein folding, proteolysis, redox regulation, cell signaling, electron transport and metabolism were found to be down-regulated in berberine-treated MCF-7 cells. In contrast, proteins known to be involved in protein trafficking were found to be up-regulated in berberine treated MCF-7 cells. Almost half of the differentially expressed proteins identified were cytosolic proteins (Supplemental Fig. 3A) and predominantly involved in gene regulation, signal transduction and the cytoskeleton (Supplemental Fig. 3B).

3.4. *Validation of proteomic results by immunoblotting and ELISA*

To validate differential expression of the identified proteins, immunoblotting and ELISA analysis were performed to compare the protein expression levels between berberine- and control-treated MCF-7 cells. In general, there was a good correlation between changes observed in the 2D-DIGE analysis and by immunoblotting/ELISA analysis. Validation confirmed the up-regulation of cytokeratin 19 (KRT19), HSP27, SLC25A23, prohibitin (PHB) and histone deacetylase 1 (HDAC1) in berberine-treated MCF-7 cells in comparison to the levels in control MCF-7 (Fig. 5A, B, C, H and I). In contrast, the down-regulation of peptidyl-prolyl cis-trans isomerase A (PPIA), peroxiredoxin 2 (PRDX2), 14-3-3 zeta and peroxiredoxin 6 (PRDX6) were confirmed as being down-regulated in response to berberine treatment (Fig. 5D, E, F and G).

3.5. *Redox proteomic analysis of berberine-induced cysteine modifications of MCF-7 proteins*

Berberine has been reported to induce cytotoxicity via ROS generation in several different cancer cell lines (see Introduction) and we confirm ROS generation in breast cancer cell line MCF-7 (Fig. 2). We thus hypothesized that berberine-induced ROS might damage or deregulate cellular proteins by oxidative modification of their cysteinyl thiol groups. Accordingly, we applied a recently developed redox 2D-DIGE methodology utilizing iodoacetylated ICy dyes [17] to assess berberine-induced changes in protein thiol reactivity. Berberine-treated (100 μg/mL) or vehicle-treated cells were lysed in the presence of ICy5 in triplicate. Individual ICy5-labeled samples were then run on 2D gels against an equal load of ICy3-labeled standard pool comprising of an equal mixture of both sample types to aid in spot matching and to improve the accuracy of quantification. The ICy5-labeled samples were subsequently labeled with

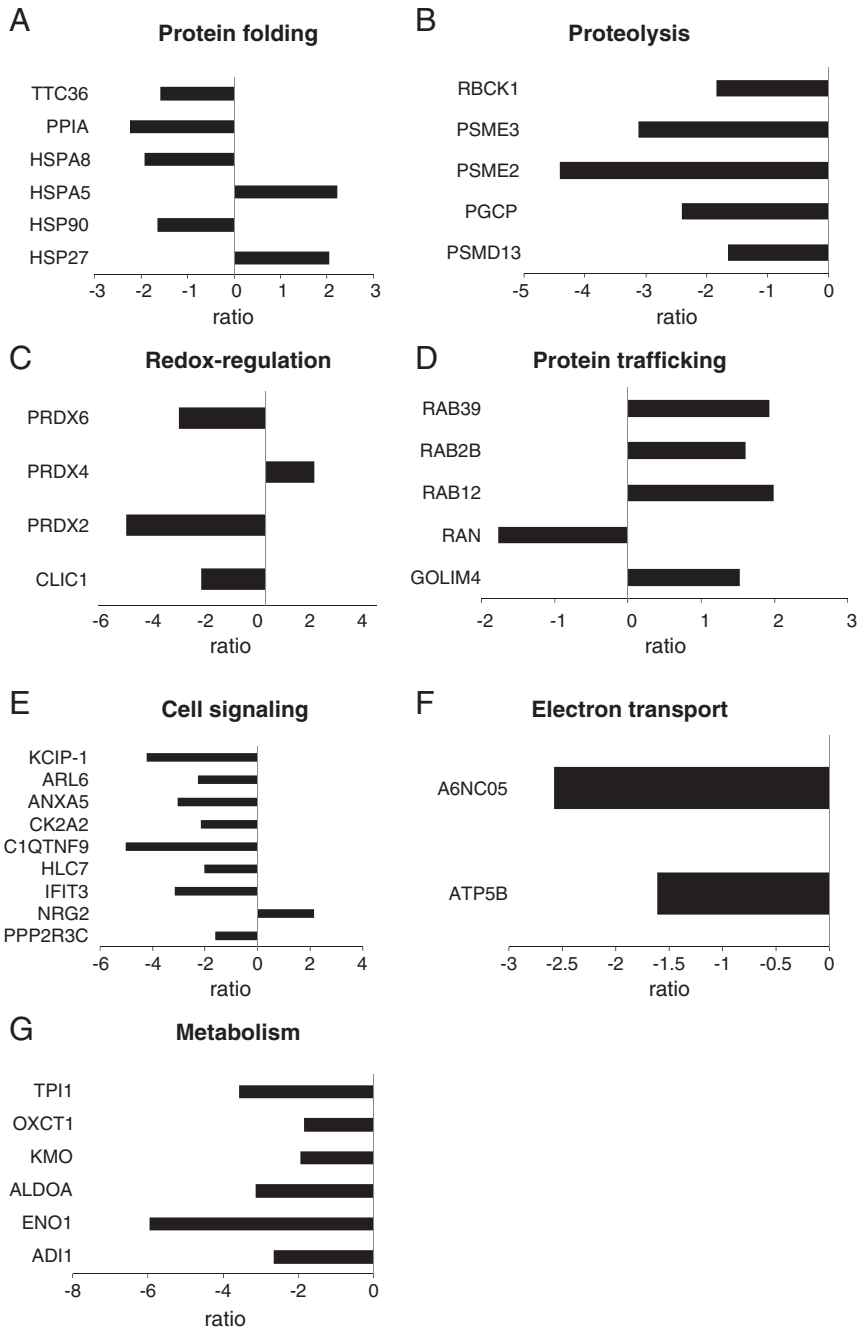

Fig. 4 – Expression profiles for differentially expressed proteins potentially contributing to: (A) protein folding, (B) proteolysis, (C) redox regulation, (D) protein trafficking, (E) cell signaling, (F) electron transport and (G) metabolism. Horizontal bars represent fold-changes in protein expression in berberine-treated versus untreated MCF-7 cells for each protein. Additional details for each protein can be found in Table 1.

lysine labeling Cy2 dye as an internal protein level control which was used to normalize the corresponding ICy5/ICy3 signals (Supplementary Fig. 4). Around 2000 protein features were detected, of which 55 displayed statistically significant differences in labeling due to berberine treatment (Fig. 6A). CCB post-staining and matching with fluorescence images allowed

Fig. 5 – Validation of berberine-induced differential protein expression by immunoblotting and enzyme-linked immunosorbent assay. The altered expression of identified proteins; (A) cytoskeletal 19, (B) HSP-27, (C) prohibitin, (D) peroxiredoxin 2, (E) PPIA, (F) peroxiredoxin 6 and (G) 14-3-3 protein zeta were assessed by immunoblotting (left panels). The protein 2D-DIGE map (right top panels) and three-dimensional spot image (right bottom panels) are also shown. ELISA analysis was performed to determine the levels of (H) histone deacetylase 1 and (I) SLC25A23 in berberine-treated versus untreated MCF-7 cells.

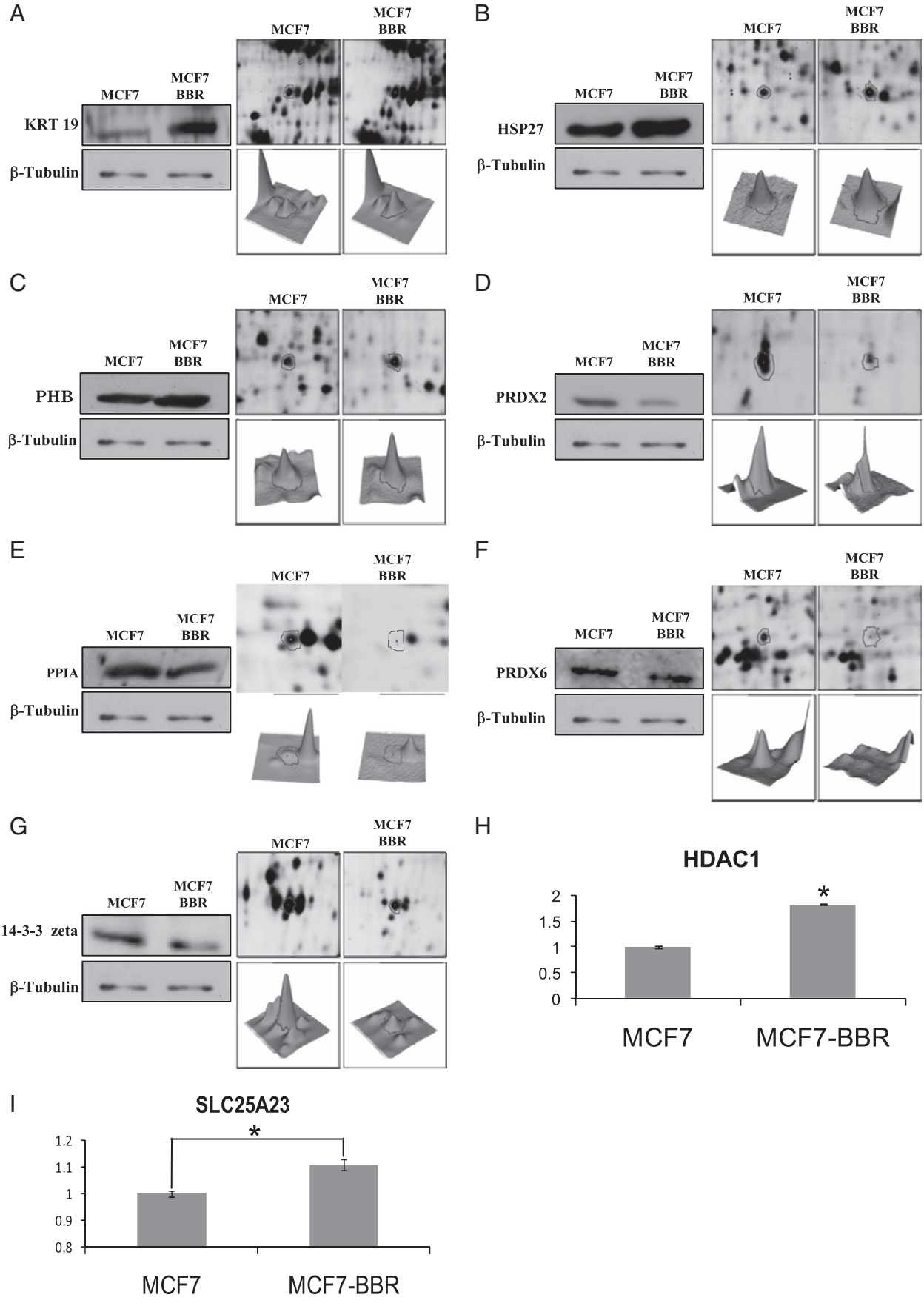
A
MCF7
MCF7 BBR
KRT 19
β-Tubulin
B
HSP27
C
PHB
D
PRDX2
E
PPIA
F
PRDX6
G
14-3-3 zeta
H
HDAC1
2
1.5
1
0.5
0
MCF7
MCF7-BBR
I
SLC25A23
1.2
1.1
1
0.9
0.8

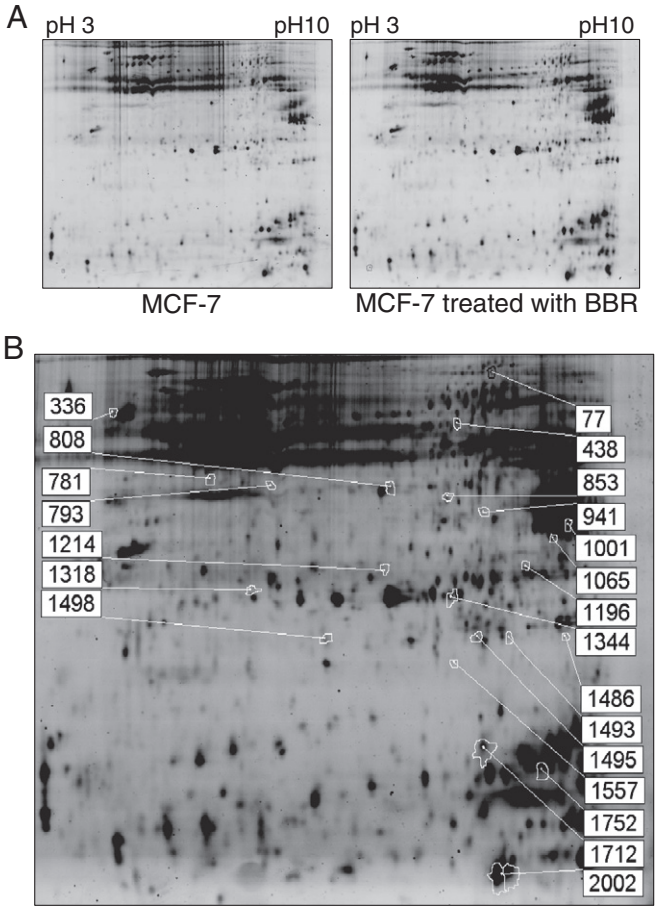

Fig. 6 – Redox 2D-DIGE analysis of berberine-induced differential cysteine-modification in MCF-7 cells. (A) Lysates from MCF-7 cells treated with 100 μg/mL of berberine or left untreated were subjected to redox 2D-DIGE analysis as described in Materials and methods. Images of protein samples from untreated and berberine-treated MCF-7 are displayed. (B) Differentially labeled protein features are annotated with spot numbers.

confident picking of 44 gel features and 22 of these were identified as unique gene products by MALDI-TOF peptide mass fingerprinting or MALDI-TOF/TOF peptide sequence analysis (Table 2, Fig. 6B and Supplementary Fig. 5). All of the identified proteins contain at least one cysteine, and since the ICy dyes target reduced cysteinyl thiols, these results suggest that berberine alters the oxidative status of some of these thiol groups. Indeed, 17 putative sites of thiol modification on 9 proteins were inferred, based on the added mass of the ICy dyes in MALDI-TOF MS spectra. The possible biological roles of these modifications are discussed below and warrant further investigation. The differentially labeled proteins were mostly cytoplasmic and fell into several functional groups including redox regulation, signal transduction, biosynthesis, protein folding and gene regulation (Supplemental Fig. 6).

3.6. *Validation of redox-induced changes in HSP27*

To validate alterations of thiol reactivity of the identified proteins, immunoprecipitation combined with immunoblotting was performed to compare the free thiol group levels and protein expression levels between berberine- and control-treated MCF-7 cells. Validation confirmed the increase of free thiol content of HSP27 and the up-regulation of HSP27 protein in berberine-treated MCF-7 cells compared to untreated cells (Fig. 7).

4. Discussion

Extensive attention has been paid to the identification of naturally occurring chemotherapeutic botanicals which are able to inhibit, delay or reverse tumorigenesis or metastasis. The assessment of ancient herbal medicines might offer a strategy for the treatment of breast cancer, which remains a primary cause of cancer-related deaths in the world [18]. In the present study, we examined the molecular mechanisms of berberine cytotoxicity in breast cancer cells *in vitro* since berberine has been shown to exhibit anti-tumorigenic ability in several different cancer types [5,7,9]. By means of 2D-DIGE and MALDI-TOF MS, more than 90 berberine-induced alterations in

Table 2 – Differential cysteine labeled proteins identified by ICy 2D-DIGE and MS. Proteins displaying berberine-induced differential labeling of cysteines and lysines using ICy dyes and NHS-Cy2 dyes, respectively, were identified by MALDI-TOF peptide mass mapping and MS/MS sequence analysis. Proteins displaying an average fold-difference of ≥1.3-fold where $P < 0.05$ and spots matched in all images are shaded gray.

No.	Swiss-prot no.	Protein name	pI	MW	Match. peptides	Cov. (%)	Score	MCF-7-ber/ MCF-7 (C)[b]	MCF-7-ber/ MCF-7 (L)[c]	MCF-7-ber/ MCF-7 (C/L)[d]	Subcellular location	Function classification	Matched peptide sequences	ICy5 containing peptide sequence	ICy3 containing peptide sequence
781	P60709	Actin, cytoplasmic 1[a]	5.29	42,052	2	33	210	–1.35	–1.26	–1.07	Cytoplasm	Cytoskeleton	K.IWHHTFYNELR.V;K.SYELPDGQVITIGNER.F	M.DDDIAALVVDNGSGMCK.A	
853	P52848	Bifunctional heparan sulfate N-deacetylase/N-sulfotransferase 1	8.07	101,488	8/12	6	62/56	–1.32	1.09	–1.34	Golgi apparatus membrane; single-pass type II membrane protein	Heparin biosynthesis	K.GDMPTLTDK.G; -.MPALACLR.R	-.MPALACLR.R	M.PALACLR.R
438	Q9NXG0	Centlein	8.28	162,143	14/17	8	85/56	1.01	–1.33	1.34	Nucleus	Mitosis	K.SSHTAVPTR.V; R.QKVNLESNK.S	R.CTDLLNDLEKLR.K; K.NCKMQK.S	
1498	Q96KP4	Cytosolic non-specific dipeptidase/Peptidase A	5.66	53,187	6/13	14	65/56	1.8	–1.23	2.21	Cytoplasm	Proteolysis	R.EGGSIPVTLTFQEATGK.N;M.AALTTLFK.Y		
1214	P30040	Endoplasmic reticulum protein ERp29/ERp29	6.77	29,032	6/12	21	65/56	–1.11	–2.02	1.82	Endoplasmic reticulum lumen	Protein folding	K.FDTQYPYGEK.Q; K.ESYPVFYLFR.D		
1493	Q99447	Ethanolamine-phosphate cytidylyltransferase	6.44	44,264	6/14	24	61/56	–1.09	1.5	–1.64	Cytoplasm	Biosynthesis	K.WVDEVVPAAPYVTTLETLDK.Y; K.ELAFLEAARQQAAQPLGER.D		R.ECKR.T
77	Q96AE4	Far upstream element-binding protein 1/FBP[a]	7.18	67,690	2	14	99	–1.02	–1.53	1.5	Nucleus	Gene regulation	R.IAQITGPPDR.C; R.GTPQQIDYAR.Q		
1196	Q14314	Fibroleukin/pT49	7.08	50,824	6/12	13	60/56	1.12	1.35	–1.43	Secreted	Immunity	K.CPSQEQIQSRPVQHLIYK.D;K.NAKEEINVLHGR.L	K.DVCPVR.L	K.DVCPVRLESR.G
1557	P30043	Flavin reductase/FR[a]	7.13	22,219	1	16	57	–1.31	1.18	–1.55	Cytoplasm	Redox regulation	K.TVAGQDAVIVLLGTR.N		
1486	P29992	Guanine nucleotide-binding protein subunit alpha-11/GNA11	5.51	42,382	8/15	21	71/56	–1.53	–1.17	–1.31	Plasma membrane	Signal transduction	K.TLWEDPGIQECYDR.R;K.IIYSHFTCATDTENIR.F	–.MTLESMMACCLSDEVK.E;M.TLESMMACCLSDEVK.E;K.TLWEDPGIQECYDR.R; M.TLESMMACCLSDEVK.E	
1318	P04792	Heat shock protein beta-1/HSP 27[a]	5.98	22,826	3	36	228	1.81	1.43	1.27	Cytoplasm	Protein folding	R.GPSWDPFR.D; R.LFDQAFGLPR.L; K.LATQSNEITIPVTFESR.A		

(continued on next page)

Table 2 (*continued*)

1065	P22626	Heterogeneous nuclear ribonucleoproteins A2/B1(hnRNP A2/B1)	8.97	37,464	5/14	22	82/56	1.02	−2.43	2.48	Nucleus	Gene regulation	R.NMGGPYGGGNYGPGGSGGSGGYGGR.S; K.LFIGGLSFETTEESLR.N		
1001	Q5JSS6	Meiosis expressed gene 1 protein homolog/MEIG1	9.14	10,845	5/12	37	57/56	−1	−1.7	1.7	Nucleus	Gene regulation	K.QVSMVDR.W;K.QVSMVDRWPETGYVK.K		
1752	P22392	Nucleoside diphosphate kinase B/NDK B[a]	8.52	17,401	3	20	138	−1.34	−1	−1.34	Cytoplasm	Biosynthesis	R.TFIAIKPDGVQR.G;K.DRPFFPGLVK.Y; R.GDFCIQVGR.N		
941	Q9NRN5	Olfactomedin-like protein 3/HNOEL-iso	6.17	46,380	6/14	13	58/56	1.38	2.1	−1.52	Secreted	Development	K.IYVLDGTQNDTAFVFPRLR.D;K.NKMLPLLEVAEK.E		
1712	Q9BZF2	Oxysterol-binding protein-related protein 7/ORP-7	8.31	96,398	8/14	13	73/56	−1.46	1.09	−1.59	Cytoplasm	Sterol signaling	R.GLPPTDYAHLQRSFWALAQK.V; K.VHSSLSSVLAALTMER.D	R.LCEELEYSSLLDQASR.I; R.CSHELSECQGK.L	R.CSHELSECQGKLQELHR.L;R.CSHELSECQGK.L
1495	Q13442	PDGF-associated protein/PDAP1/28 kDa heat- and acid-stable phosphoprotein[a]	8.84	20,618	1	7	58	1.01	−1.54	1.56	Cytoplasm	Signal transduction	K.GVEGLIDIENPNR.V		
336	P07237	Protein disulfide-isomerase/PDI/p55	4.76	57,480	9/23	20	87/56	−1.71	−1.82	1.06	Endoplasmic reticulum lumen; melanosome; cell membrane; peripheral membrane protein	Protein folding	K.YQLDKDGVVLFK.K; K.VDATEESDLAQQYGVR.G		
793	Q7Z628	Proto-oncogene p65 Net1/Neuroepithelial cell-transforming gene 1 protein	9.31	68,154	8/20	16	57/56	1.41	1.02	1.38	Cytoplasm and nucleus	Signal transduction	R.VTSLANLISPVR.N; R.CGSGMQMAEDSKSLK.T	R.CSLRR.G;R.CGSGMQMAEDSKSLK.T	R.GYCSNQLAAKALLDQK.K
2002	Q6NV95	Putative protein PABPC1-like	8.88	30,256	5/9	25	58/56	−1.51	−1.65	1.09	Nucleus	Gene regulation	R.LAHFTNQYMQKMASVR.A;K.RFGFVCFSSPEEVAK.A	K.RFGFVCFSSPEEVAK.A	
808	Q9Y6N5	Sulfide:quinone oxidoreductase, mitochondrial	9.18	50,214	7/22	13	77/56	−1.03	1.51	−1.56	Mitochondrion	Redox regulation	K.ERLSMYLMK.A; R.TISVIMK.N		
1344	P60174	Triosephosphate isomerase/TIM/TPI1[a]	6.45	26,938	2	37	281	−1.1	1.27	−1.4	Cytoplasm	Glycolysis	K.FFVGGNWK.M;K.VPADTEVVCAPPTAYIDFAR.Q		

[a]Proteins identified by MALDI-TOF/TOF.

[b]Average fold-differences of triplicate samples run on different gels from DeCyder analysis show cysteine-labeling ratios (C) for berberine-treated versus untreated MCF-7 cells. Here, the ICy5 signal was used to monitor cysteine-labeling alterations against ICy3 signals used as an internal standard.

[c]Average fold-differences of triplicate samples run on different gels from DeCyder analysis show lysine-labeling ratios (L) for berberine-treated versus untreated MCF-7 cells. Here, the NHS-Cy2 signal was used to monitor lysine-labeling alterations against ICy3 signals used as an internal standard.

[d]To accurately calculate berberine-induced differential labeling of cysteines in consideration of protein level alterations, the cysteine-labeling ratio (C) was normalized using the lysine-labeling ratio (L).

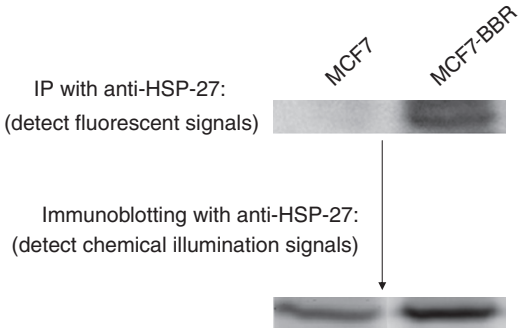

Fig. 7 – Validation of the thiol reactive protein, HSP-27, identified through redox-proteomic study in MCF-7 cells after berberine treatment by IP-WB. ICy dye-labeled protein samples from MCF-7 cells were either untreated or treated with 100 μg/mL of berberine followed by immunoprecipitated with HSP-27 antibody to confirm the alterations of thiol reactivity in HSP-27. The image was visualized by Ettan DIGE imager. Immunoblotting against the corresponding antibody was performed to gain the protein level.

protein expression have been identified in MCF-7 cells. The results demonstrate that this strategy is powerful enough to identify a broad-ranging signature of berberine-induced cytotoxicity, with the altered proteins having roles in gene regulation, signal transduction, cytoskeleton regulation and metabolism. Even though the global coverage of protein mixtures identified by LC-MS based analysis is generally recognized to be higher than that of 2-DE based analysis, 2-DE based analysis offers the advantage of direct protein quantification at the protein isoform level with reduced analytical variation [11]. Our study also revealed that treatment of breast cancer cells with berberine results in the generation of reactive oxygen species. Since ROS can activate signaling pathways, modulate a variety of cellular activities and regulate disease progression, it is important to study the molecular events associated with their effects. Accordingly, our previously established cysteine-labeling 2D-DIGE platform using ICy3/ICy5 dyes was thus used to determine if protein thiol reactivity is altered in cells following treatment with berberine due to ROS generation.

Our studies using MCF-7 cells as an *in vitro* model demonstrated that treatment with berberine leads to decreased cell viability at least partially through the over-expression of p53 and p21 and blockade of Bcl-2 expression. In addition, proteomic analysis revealed that HDAC1, a key negative regulator of eukaryotic gene expression, was up-regulated in response to berberine treatment [19]. HDAC1 interacts with the retinoblastoma tumor-suppressor protein, and deacetylates p53 and histones to modulate cell growth and apoptosis [20–22]. Thus, the up-regulation of HDAC1 may contribute to berberine-induced apoptosis of breast cancer cells through its deacetylation activity. Another identified cell survival modulator protein was serine/threonine-protein phosphatase 2A, which was increased 8-fold during berberine treatment. Since serine/threonine-protein phosphatase 2A activation has been reported to trigger the dephosphorylation of Bad and subsequent interaction with Bcl-XL resulting in the initiation of apoptosis [23,24], we propose that berberine may promote cell death in MCF-7 cells via the over-expression of serine/threonine-protein phosphatase 2A. Moreover, the up-regulation of prohibitin, a repressor of E2F-mediated DNA synthesis and cellular proliferation [25], may also contribute to the observed berberine-induced loss of viability in these cells, as may the observed down-regulation of 14-3-3 zeta, a positive regulator of cell proliferation, whose overexpression in mammary epithelial cells has been shown to disrupt apoptotic signaling by down-regulating p53 [26].

Our proteomic analysis revealed berberine to down-regulate the majority (63%) of identified proteins which are involved in a variety of cellular processes including protein folding, redox regulation, gene regulation and signal transduction. We hypothesize that berberine may interfere with the proper folding of cellular proteins through the reduced expression of chaperone and folding proteins such as HSP90, GRP78 and PPIA, and that this may be linked to a general stress response. Notably, peptidyl-prolyl cis-trans isomerase A has been described to be able to inhibit procaspase-3 activation by sequestering cytochrome c [27]. It is tempting to speculate that berberine might trigger apoptosis of MCF-7 cells at least partially via the down-regulation of peptidyl-prolyl cis-trans isomerase A. Mitochondria are well-known to play a key role in regulating cellular apoptosis [28] and recent reports indicate that berberine inhibits mitochondrial electron transport [29] and induces apoptosis through a mitochondria/caspase-dependent pathway in human hepatoma cells [30]. The down-regulation of mitochondrial electron transport proteins in the present study appears to support this.

Notably, all of the identified proteins with roles in metabolism (chiefly glycolytic enzymes) were found to be down-regulated, suggesting interplay between berberine-induced apoptosis and metabolism in breast cancer. Indeed, it has been previously reported that the pro-apoptotic Bcl-2 family member BAD, resides in a glucokinase-containing complex in the mitochondrion that regulates glucose-driven mitochondrial respiration and cell death dependent upon glucose availability [31,32]. Thus, berberine might deregulate glycolysis in MCF-7 cells via its effect on pro-apoptotic proteins such as BAD. Importantly, the identified glycolytic enzymes; triosephosphate isomerase, fructose-bisphosphate aldolase A and alpha-enolase, displayed significant down-regulation, also supporting previous data showing that oxidative stress can redirect carbohydrate fluxes to generate increased reducing power in the form of NADPH at the expense of glycolysis [33,34].

Berberine has been widely reported to induce ROS which are important mediators of attenuated tumor growth and cancer cell apoptosis [35–39]. These processes are mediated by increasing endoplasmic reticulum stress, promoting the expression of caspases, blocking the G2/M checkpoint, reducing mitochondrial potential and activation of JNK and p38 MAPK signaling pathways. Our present data supports the idea that berberine can also induce cell death in MCF-7 cells through the generation of ROS. However, a recent report suggested the opposite, where berberine inhibited the production of ROS in LPS-stimulated macrophages via inhibition of NADPH oxidase [40]. Additionally, berberine has been shown to decrease

lysophosphatidylcholine-stimulated vascular smooth muscle cell proliferation via inhibition of ROS generation through inactivation of the ERK1/2 pathway [41]. We thus propose that berberine might have multiple cellular targets and distinct effects that may be cell type and context specific. For example, in fast-growing human colon cancer, berberine might target JNK/p38 signaling to induce apoptosis through the generation of ROS. In contrast, in macrophages, the highly active NADPH oxidase becomes a dominant cellular target of berberine with the inactivation of NADPH oxidase leading to diminished production of ROS.

ROS are known to modify protein cysteinyl thiol groups, resulting in oxidative damage [42–44]. We therefore applied a recently developed 2D-DIGE methodology utilizing iodoacetyl ICy dyes to assess berberine-induced changes in the thiol reactivity of cellular proteins in MCF-7 cells. Individual ICy5- and Cy2-labeled samples were run on 2D gels against an equal load of an ICy3-labeled standard pool consisting of an equal mixture of the differentially treated samples to accurately determine changes in the thiol reactivity of the proteins. This novel strategy accurately quantified changes of thiol reactivity of cysteine residues taking into consideration variation due to protein expression change (Supplementary Fig. 4).

The ICy labeling data presented supports the hypothesis that berberine can induce the formation of free thiols in certain proteins through disruption of disulphide bonds; meanwhile, berberine induced ROS or protein-derived peroxides may directly oxidize thiol groups to form the sulfenic, sulfinic or sulfonic acid forms of cysteine, which would not react with the ICy dyes. These thiol modifications have been reported to perturb the normal functions of the proteins [45]. In the current study, twenty-two proteins with differential thiol reactivity were identified by MALDI-TOF and/or MALDI-TOF/TOF. Centlein, neuroepithelial cell transforming gene 1 protein (NET1), far upstream element-binding protein 1 (FUBP1) and PDGFA-associated protein 1 (PDAP1) are reported to maintain cell proliferation and survival and all displayed an increase in ICy dye labeling following berberine treatment (Table 2). Thus, their cysteine residues must be reduced to generate new thiol groups for ICy labeling, implying possible oxidative damage and deregulation of these proteins. Centlein plays an important role in duplication of centrioles and might modulate the molecular function of the centrosome [46]; a critical organelle that controls G2/M checkpoint transition in the cell cycle [47]. Thus, we proposed that the oxidative modification of centlein may result in centrosome dysfunction during cell cycle progression and possibly lead to cell apoptosis. The proto-oncogene NET1 is a Rho guanine nucleotide exchange factor for RhoA and has been reported to be able to activate the SAPK/JNK pathway via a RhoA-independent pathway [48]. SAPK/JNK pathway activation can induce expression of the Fas death receptor to promote apoptotic cell death [49]. It will be important to assess directly the consequences of redox modification on NET1 function. In contrast, several of the identified proteins, such as GNA11, NDK B, ORP-7 and TPI1, displayed a decrease in ICy dye labeling following berberine treatment (Table 2). Thus, their free thiol groups must be oxidized in response to berberine treatment to block ICy labeling, implying possible oxidative damage and deregulation of these proteins. GNA11, a subunit of heterotrimeric G proteins, can transduce extracellular signals received by transmembrane receptors to intracellular effector proteins such as phospholipase C [50]. GNA11 is associated with the plasma membrane via palmitoylation of the N-terminal region of the protein which plays a key role in interactions of the G-protein with receptors and effectors. McCallum et al. reported that mutations of Cys-9 and Cys-l0 potentially interfered with

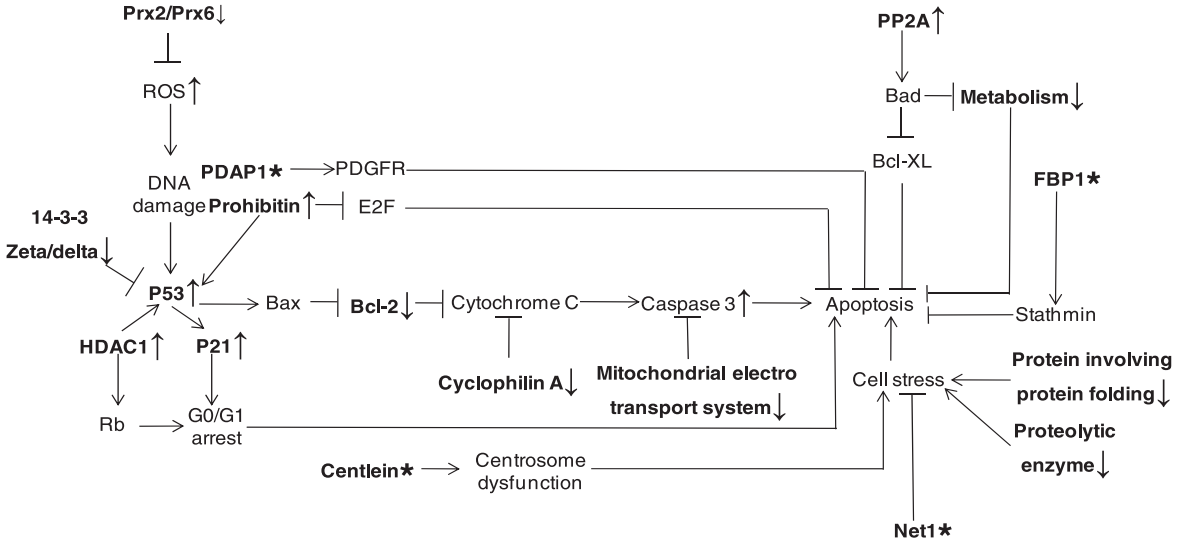

Fig. 8 – Model of berberine-induced cell apoptosis. Mechanisms of berberine-induced breast cancer cell toxicity and apoptosis are proposed. The proposed mechanisms suggest p53-induction as an important cellular target of berberine treatment. Berberine-induced protein damage may promote apoptosis via p53-independent pathways. Identified proteins and pathways involved in this network are highlighted in bold. Identified proteins that were up-regulated and down-regulated in response to berberine treatment are denoted with "↑" and "↓", respectively. Proteins with possible redox-modifications are denoted with "*".

lipidation of the protein [51]. In our current study, we observed a decreased labeling of GNA11 protein and putatively identified ICy5-modified peptides at Cys-9 or Cys-10 of GNA11 by MALDI-TOF MS. These results imply that berberine treatment might interfere with the palmitoylation and association of GNA11 with the plasma membrane to disrupt its signaling activity.

In conclusion, the present study offers an insight into the mechanisms of berberine-induced apoptosis in human breast cancer cells and shows a link between ROS generation and the cell death process. The proposed mechanisms of berberine-induced cell death are summarized in Fig. 8. The findings of this study may have clinical implications in that berberine treatment may be useful in destroying fast-growing cancer cells with limited toxicity to normal cells. Additionally, numerous identified cellular proteins may be useful for further evaluation as potential targets in breast cancer therapy.

Acknowledgments

This work was supported by NSC grant (100-2311-B-007-005) from National Science Council, Taiwan, and Nano- and Micro-ElectroMechanical Systems-based Frontier Research on Cancer Mechanism, Diagnosis, and Treatment grant from National Tsing Hua University. The authors also thank CMU-NTHU Joint Research grant no. 98N2443E1.

Appendix A. Supplementary data

Supplementary data to this article can be found online at doi:10.1016/j.jprot.2012.03.010.

REFERENCES

[1] Jantova S, Cipak L, Cernakova M, Kost'alova D. Effect of berberine on proliferation, cell cycle and apoptosis in HeLa and L1210 cells. J Pharm Pharmacol 2003;55:1143–9.
[2] Kuo CL, Chi CW, Liu TY. Modulation of apoptosis by berberine through inhibition of cyclooxygenase-2 and Mcl-1 expression in oral cancer cells. In Vivo 2005;19:247–52.
[3] Wu M, Wang J, Liu LT. Advance of studies on anti-atherosclerosis mechanism of berberine. Chin J Integr Med 2010;16:188–92.
[4] Johnson CC, Johnson G, Poe CF. Toxicity of alkaloids to certain bacteria. II. Berberine, physostigmine, and sanguinarine. Acta Pharmacol Toxicol (Copenh) 1952;8:71–8.
[5] Tan YL, Goh D, Ong ES. Investigation of differentially expressed proteins due to the inhibitory effects of berberine in human liver cancer cell line HepG2. Mol Biosyst 2006;2:250–8.
[6] Iizuka N, Miyamoto K, Okita K, Tangoku A, Hayashi H, Yosino S, et al. Inhibitory effect of Coptidis Rhizoma and berberine on the proliferation of human esophageal cancer cell lines. Cancer Lett 2000;148:19–25.
[7] Wu K, Yang Q, Mu Y, Zhou L, Liu Y, Zhou Q, et al. Berberine inhibits the proliferation of colon cancer cells by inactivating Wnt/beta-catenin signaling. Int J Oncol 2012;41:292–8, doi:10.3892/ijo.2012.1423.
[8] Kim JB, Lee KM, Ko E, Han W, Lee JE, Shin I, et al. Berberine inhibits growth of the breast cancer cell lines MCF-7 and MDA-MB-231. Planta Med 2008;74:39–42.
[9] Meeran SM, Katiyar S, Katiyar SK. Berberine-induced apoptosis in human prostate cancer cells is initiated by reactive oxygen species generation. Toxicol Appl Pharmacol 2008;229:33–43.
[10] Peng PL, Hsieh YS, Wang CJ, Hsu JL, Chou FP. Inhibitory effect of berberine on the invasion of human lung cancer cells via decreased productions of urokinase-plasminogen activator and matrix metalloproteinase-2. Toxicol Appl Pharmacol 2006;214:8–15.
[11] Timms JF, Cramer R. Difference gel electrophoresis. Proteomics 2008;8:4886–97.
[12] Hung PH, Chen YW, Cheng KC, Chou HC, Lyu PC, Lu YC, et al. Plasma proteomic analysis of the critical limb ischemia markers in diabetic patients with hemodialysis. Mol Biosyst 2011;7:1990–8.
[13] Huang HL, Hsing HW, Lai TC, Chen YW, Lee TR, Chan HT, et al. Trypsin-induced proteome alteration during cell subculture in mammalian cells. J Biomed Sci 2010;17:36.
[14] Chou HC, Chen YW, Lee TR, Wu FS, Chan HT, Lyu PC, et al. Proteomics study of oxidative stress and Src kinase inhibition in H9C2 cardiomyocytes: a cell model of heart ischemia reperfusion injury and treatment. Free Radic Biol Med 2010;49:96–108.
[15] Chan HL, Gharbi S, Gaffney PR, Cramer R, Waterfield MD, Timms JF. Proteomic analysis of redox- and ErbB2-dependent changes in mammary luminal epithelial cells using cysteine- and lysine-labelling two-dimensional difference gel electrophoresis. Proteomics 2005;5:2908–26.
[16] Lai TC, Chou HC, Chen YW, Lee TR, Chan HT, Shen HH, et al. Secretomic and proteomic analysis of potential breast cancer markers by two-dimensional differential gel electrophoresis. J Proteome Res 2010;9:1302–22.
[17] Chan HL, Gaffney PR, Waterfield MD, Anderle H, Peter MH, Schwarz HP, et al. Proteomic analysis of UVC irradiation-induced damage of plasma proteins: serum amyloid P component as a major target of photolysis. FEBS Lett 2006;580:3229–36.
[18] Hackshaw AK, Paul EA. Breast self-examination and death from breast cancer: a meta-analysis. Br J Cancer 2003;88:1047–53.
[19] Cai RL, Yan-Neale Y, Cueto MA, Xu H, Cohen D. HDAC1, a histone deacetylase, forms a complex with Hus1 and Rad9, two G2/M checkpoint Rad proteins. J Biol Chem 2000;275:27909–16.
[20] Giacinti C, Giordano A. RB and cell cycle progression. Oncogene 2006;25:5220–7.
[21] Wade PA. Transcriptional control at regulatory checkpoints by histone deacetylases: molecular connections between cancer and chromatin. Hum Mol Genet 2001;10:693–8.
[22] Gu W, Luo J, Brooks CL, Nikolaev AY, Li M. Dynamics of the p53 acetylation pathway. Novartis Found Symp 2004;259:197–205.
[23] Garcia A, Cayla X, Guergnon J, Dessauge F, Hospital V, Rebollo MP, et al. Serine/threonine protein phosphatases PP1 and PP2A are key players in apoptosis. Biochimie 2003;85:721–6.
[24] Klumpp S, Krieglstein J. Serine/threonine protein phosphatases in apoptosis. Curr Opin Pharmacol 2002;2:458–62.
[25] McClung JK, Jupe ER, Liu XT, Dell'Orco RT. Prohibitin: potential role in senescence, development, and tumor suppression. Exp Gerontol 1995;30:99–124.
[26] Danes CG, Wyszomierski SL, Lu J, Neal CL, Yang W, Yu D. 14-3-3 zeta down-regulates p53 in mammary epithelial cells and confers luminal filling. Cancer Res 2008;68:1760–7.
[27] Bonfils C, Bec N, Larroque C, Del Rio M, Gongora C, Pugniere M, et al. Cyclophilin A as negative regulator of apoptosis by sequestering cytochrome c. Biochem Biophys Res Commun 2010;393:325–30.

[28] Wang C, Youle RJ. The role of mitochondria in apoptosis*. Annu Rev Genet 2009;43:95–118.
[29] Turner N, Li JY, Gosby A, To SW, Cheng Z, Miyoshi H, et al. Berberine and its more biologically available derivative, dihydroberberine, inhibit mitochondrial respiratory complex I: a mechanism for the action of berberine to activate AMP-activated protein kinase and improve insulin action. Diabetes 2008;57:1414–8.
[30] Hwang JM, Kuo HC, Tseng TH, Liu JY, Chu CY. Berberine induces apoptosis through a mitochondria/caspases pathway in human hepatoma cells. Arch Toxicol 2006;80:62–73.
[31] Danial NN, Walensky LD, Zhang CY, Choi CS, Fisher JK, Molina AJ, et al. Dual role of proapoptotic BAD in insulin secretion and beta cell survival. Nat Med 2008;14:144–53.
[32] Danial NN, Gramm CF, Scorrano L, Zhang CY, Krauss S, Ranger AM, et al. BAD and glucokinase reside in a mitochondrial complex that integrates glycolysis and apoptosis. Nature 2003;424:952–6.
[33] Shenton D, Grant CM. Protein S-thiolation targets glycolysis and protein synthesis in response to oxidative stress in the yeast *Saccharomyces cerevisiae*. Biochem J 2003;374:513–9.
[34] Weeks ME, Sinclair J, Butt A, Chung YL, Worthington JL, Wilkinson CR, et al. A parallel proteomic and metabolomic analysis of the hydrogen peroxide- and Sty1p-dependent stress response in *Schizosaccharomyces pombe*. Proteomics 2006;6:2772–96.
[35] Eom KS, Kim HJ, So HS, Park R, Kim TY. Berberine-induced apoptosis in human glioblastoma T98G cells is mediated by endoplasmic reticulum stress accompanying reactive oxygen species and mitochondrial dysfunction. Biol Pharm Bull 2010;33:1644–9.
[36] Ho YT, Lu CC, Yang JS, Chiang JH, Li TC, Ip SW, et al. Berberine induced apoptosis via promoting the expression of caspase-8, -9 and -3, apoptosis-inducing factor and endonuclease G in SCC-4 human tongue squamous carcinoma cancer cells. Anticancer Res 2009;29:4063–70.
[37] Chen TC, Lai KC, Yang JS, Liao CL, Hsia TC, Chen GW, et al. Involvement of reactive oxygen species and caspase-dependent pathway in berberine-induced cell cycle arrest and apoptosis in C6 rat glioma cells. Int J Oncol 2009;34: 1681–90.
[38] Lin CC, Yang JS, Chen JT, Fan S, Yu FS, Yang JL, et al. Berberine induces apoptosis in human HSC-3 oral cancer cells via simultaneous activation of the death receptor-mediated and mitochondrial pathway. Anticancer Res 2007;27:3371–8.
[39] Hsu WH, Hsieh YS, Kuo HC, Teng CY, Huang HI, Wang CJ, et al. Berberine induces apoptosis in SW620 human colonic carcinoma cells through generation of reactive oxygen species and activation of JNK/p38 MAPK and FasL. Arch Toxicol 2007;81:719–28.
[40] Sarna LK, Wu N, Hwang SY, Siow YL, O K. Berberine inhibits NADPH oxidase mediated superoxide anion production in macrophages. Can J Physiol Pharmacol 2010;88:369–78.
[41] Cho BJ, Im EK, Kwon JH, Lee KH, Shin HJ, Oh J, et al. Berberine inhibits the production of lysophosphatidylcholine-induced reactive oxygen species and the ERK1/2 pathway in vascular smooth muscle cells. Mol Cells 2005;20:429–34.
[42] Kemp M, Go YM, Jones DP. Nonequilibrium thermodynamics of thiol/disulfide redox systems: a perspective on redox systems biology. Free Radic Biol Med 2008;44:921–37.
[43] Cross JV, Templeton DJ. Regulation of signal transduction through protein cysteine oxidation. Antioxid Redox Signal 2006;8:1819–27.
[44] Moran LK, Gutteridge JM, Quinlan GJ. Thiols in cellular redox signalling and control. Curr Med Chem 2001;8:763–72.
[45] Ghezzi P, Bonetto V, Fratelli M. Thiol-disulfide balance: from the concept of oxidative stress to that of redox regulation. Antioxid Redox Signal 2005;7:964–72.
[46] Makino K, Umeda K, Uezu A, Hiragami Y, Sakamoto T, Ihn H, et al. Identification and characterization of the novel centrosomal protein centlein. Biochem Biophys Res Commun 2008;366:958–62.
[47] Wang Y, Ji P, Liu J, Broaddus RR, Xue F, Zhang W. Centrosome-associated regulators of the G(2)/M checkpoint as targets for cancer therapy. Mol Cancer 2009;8:8.
[48] Alberts AS, Treisman R. Activation of RhoA and SAPK/JNK signalling pathways by the RhoA-specific exchange factor mNET1. EMBO J 1998;17:4075–85.
[49] Kuwabara M, Takahashi K, Inanami O. Induction of apoptosis through the activation of SAPK/JNK followed by the expression of death receptor Fas in X-irradiated cells. J Radiat Res (Tokyo) 2003;44:203–9.
[50] Wilkie TM, Gilbert DJ, Olsen AS, Chen XN, Amatruda TT, Korenberg JR, et al. Evolution of the mammalian G protein alpha subunit multigene family. Nat Genet 1992;1:85–91.
[51] McCallum JF, Wise A, Grassie MA, Magee AI, Guzzi F, Parenti M, et al. The role of palmitoylation of the guanine nucleotide binding protein G11 alpha in defining interaction with the plasma membrane. Biochem J 1995;310(Pt 3):1021–7.